TNO innovation for life

Investigation of the Aalma el-Chaab incident

TNO Public ⟩ TNO 2023 R12286
26 January 2024

Defence, Safety & Security
www.tno.nl
+31 88 866 80 00
info@tno.nl

TNO 2023 R12286 – 26 January 2024

Investigation of the Aalma el-Chaab incident

Author(s)	Not disclosed
Classification report	TNO Public
Report text	TNO Public
Number of pages	70 (excl. front and back cover)
Sponsor	Reuters News & Media Limited
Project name	Reuters investigation

Contents

1 Introduction

On 13 October 2023, a group of journalists was struck by ammunition on a hilltop near the village of Aalma el-Chaab in southern Lebanon, close to the demarcation line between Lebanon and Israel, also referred to as the United Nations (UN) 2000 Blue Line. A visuals journalist from Reuters, Issam Abdallah, was killed and two other Reuters journalists, Thaer Al-Sudani and Maher Nazeh, were injured. Photographer Christina Assi and video journalist Dylan Collins from Agence France-Presse (AFP), and Carmen Joukhadar and Elie Brakhia from Al Jazeera were also injured in the incident [CNN, 2023].

Reuters requested an analysis of the incident by TNO, being an independent research organization established under Dutch law. The evidence collected and supplied by Reuters to TNO includes:

- fragments retrieved from the ground and from the Reuters vehicle;
- flak vests of Issam Abdallah and two other journalists;
- a camera and tripod;
- video recordings and photographs taken prior the incident;
- video recordings at the scene from Reuters, AFP, Al Jazeera during the incident;
- video recording at a distance from Radiotelevisione Italiana (RAI) during the incident;
- video recordings and photographs taken after the incident;
- MAXAR satellite images;
- autopsy report of Issam Abdallah;
- witness accounts.

To ensure an independent analysis, the investigation by TNO is based on the raw materials directly involved in the incident, i.e., the hardware and imagery as detailed above. References to imagery are included in the report text using identification information as received. The autopsy report and witness accounts are excluded from the analysis as TNO cannot guarantee their accuracy.

The analysis is conducted by seven employees of the TNO Energetic Materials Department and one employee of the Acoustics Department. The resulting report is peer-reviewed by three employees of the Explosions, Ballistics and Protection Department, then reviewed by a Senior Scientist and finally reviewed by the TNO Defence, Safety & Security Director of Science (Principal Scientist).

The objectives of the investigation include a reconstruction of the course of events, determination of firing point and identification of the ammunition articles and weapons used. These objectives are respectively described in chapter 2, 3 and 4. Chapter 5 presents the conclusions.

The scene of an ammunition strike is inherently complicated as it generally involves significant destruction of the impacted area and of the ammunition article itself. Conclusions will accordingly be based on factual findings beyond any reasonable doubt. It will be explicitly stated where ambiguity exists.

2 Course of events

From a hilltop near the village of Aalma el-Chaab, in the afternoon of 13 October 2023, journalists from Reuters, Al Jazeera and AFP are filming the smoke billowing from behind the hill to the south resulting from exploding ammunitions, see Figure 1. The journalists are wearing helmets and flak vests labelled “Press” on the front side, back side or both. A white unmarked car from Al Jazeera is parked next to the road. A bit further up the hill a car from Reuters is parked next to the road (not visible in Figure 1). The location of the journalists and main filming direction are shown in Figure 2.

Figure 1 Journalists from Reuters, Al Jazeera and AFP near the village of Aalma el-Chaab [ISSAM01.jpg].

The time at which the photo in Figure 1 has been taken is unknown, but, based on alternative footage, estimated to be approximately forty-five minutes before the incident. The time of the sequence of events leading up to the incident has been derived from the data stream (codec) of the AFP footage. At 17:10 AFP is filming the same plumes of smoke from the same location as shown in Figure 1 [C6337.MP4][1]. The sound of one or more drones can be heard. At 17:13, AFP initially films the same plumes of smoke [C6338 - AFP Footage to the East 1.MP4]. After about one minute, at 17:14, the white car is reparked to the back with the front right wheel on the asphalt. After three minutes and thirty-five seconds, at 17:16:35, the camera vibrates which is probably caused by somebody touching the camera[2]. Two and three seconds later, at 17:16:38 and 17:16:39, two near simultaneous sounds are heard thought to relate to firing and detonation of ammunition. Within three seconds, at 17:16:41, the camera starts swivelling to the southeast, where plumes of smoke resulting from the firing and detonation of ammunition are observed.

[1] The time stamp of C6337.MP4 is 15:02 in Greenwich Mean Time (GMT). The time in Aalma el-Chaab is GMT +3 hours. The actual time is corrected by adding 8 minutes to bring it in line with RAI footage [ISSAM ABDALLAH .mxf] which captured the second strike at 18:02 local time.
[2] A similar sound occurs around 0:30 in [C6339 - AFP Footage to the East 2.MP4] when the camera is redirected.

The sound of one or more drones is heard throughout the entire video clip. Stills from the video recordings made by AFP and Issam Abdallah towards the southeast are shown in Figure 3 and Figure 4. Based on audible sirens in the background, TNO has established that these video recordings overlap in time. In Figure 4, the smoke plume from the firing of ammunition is observed. In both figures the UN 2000 Blue Line and a radio tower, seen in the back, are indicated as landmarks.

Figure 2 Location of journalists and main filming direction from 17:10 to 17:16:46. The white house seen in Figure 1 is encircled [Google maps].

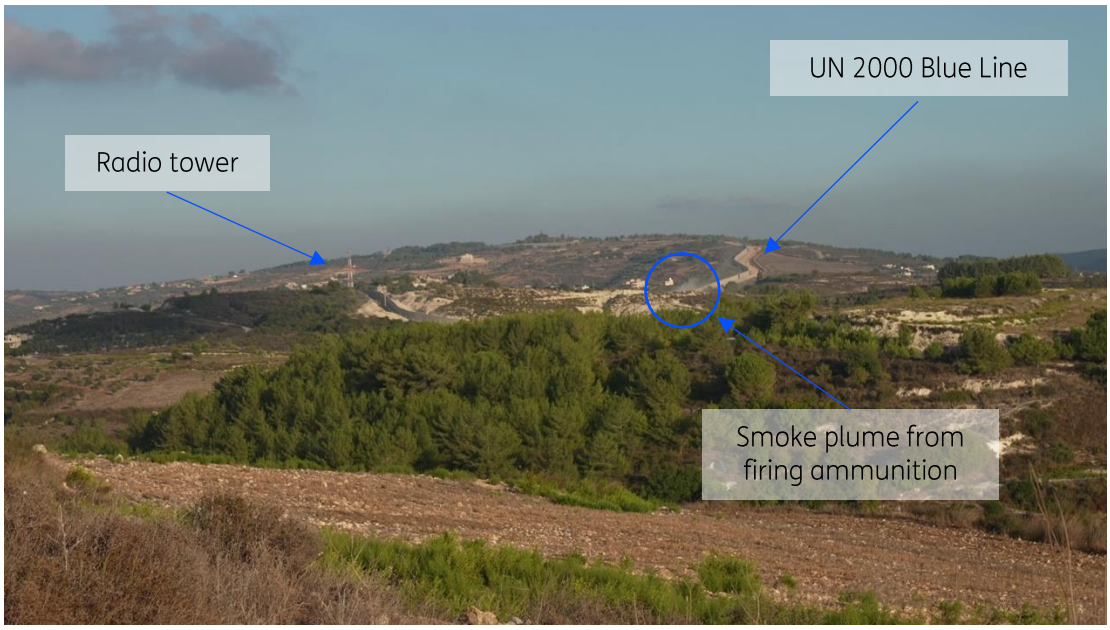

Figure 3 Still from [AFP C6338 Footage to the East 1.MP4] at 17:08:46.

Figure 4 Still from [ISSAM09.mp4], at about 17:17. The car is parked with the right front wheel on the asphalt.

The approximate main filming directions in Figure 3 and Figure 4 are presented in Figure 5, combined with the UN 2000 Blue Line and radio tower landmarks.

At 17:17, the AFP video [C6339 - AFP Footage to the East 2.MP4] initially shows the same plumes of smoke as visible in Figure 3 and Figure 4. After twenty seconds a man is heard saying “that was outgoing” and a woman is heard saying “are we safe here?”, to which the man responds with “good question”. After thirty-five seconds, at 17:17:35, the camera turns back to the south. Sirens are heard from between 17:17:50 and 17:18:30. Then sporadic distant explosions and the sound of a drone can be heard until the end of the clip at 17:20:41. At 17:34, the next AFP video [C6347.MP4] films heavy smoke plumes to the south. The distant sound of a helicopter is heard at the beginning of the clip. Between 17:36 and 17:38 artillery rounds are fired and detonating to the south, significantly increasing the smoke plumes behind the ridge that is shown in the distance in Figure 1.

After that, other distant explosions and the sound of a drone are heard. Near the end of the clip at 17:49:22 the distant sound of a helicopter is again heard[3].

Figure 5 Location of journalists and main filming direction in Figure 3 an Figure 4 at about 17:17. The UN 2000 Blue Line and Radio tower are indicated [Google Maps].

At 17:50, the AFP video [C6351.MP4] also films smoke to the south. The sound of a drone is heard, as well as the firing and detonation of an artillery round. The clip ends at 17:51:04. At 17:52, the AFP video [C6532.MP4] records the sound of a drone and several artillery rounds being fired and detonating to the south for nearly three minutes. At 17:55, the AFP video [C6353.MP4] also records the sound of a drone and the firing and detonation of artillery rounds until 17:56:05.

The incident occurs several minutes later and is recorded by a live feed recording of Reuters [Issam live footage.mp4], a recording by Al Jazeera [Al Jazeera footage. Helicopter, both strikes.mp4] and by AFP [AFP Footage.mp4]. At the time of the incident all cameras are directed southwest at an Israeli military position near the Hasulam Cave. The distance between the journalists on the hilltop and the cave is approximately 2.2 km, see Figure 6.

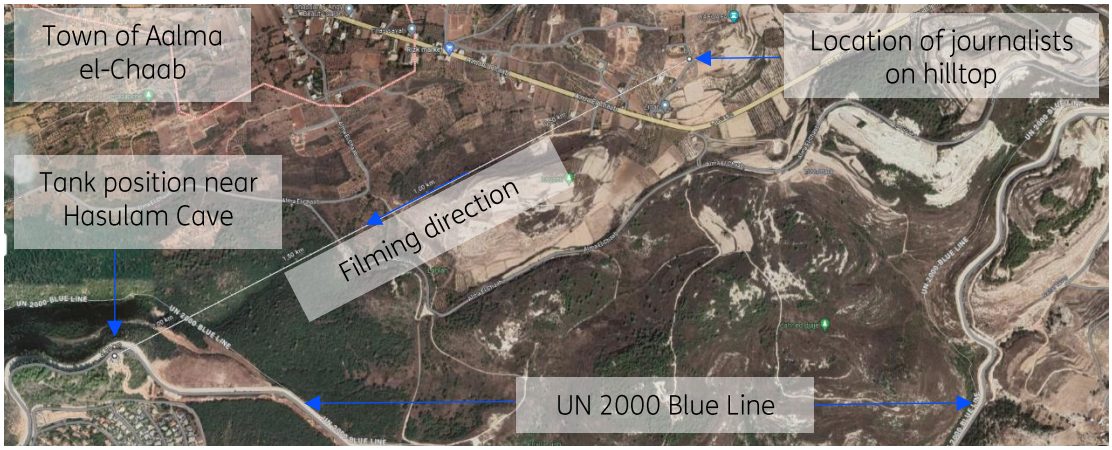

Figure 6 Location of cameras and main filming direction, tank position, UN 2000 Blue Line, near the town of Aalma el-Chaab.

[3] Based on its silhouette the helicopter is identified in [Al Jazeera footage. Helicopter, both strikes.mp4] as an Apache.

The live feed recording of Reuters [Issam live footage.mp4] and the AFP footage [AFP Footage.mp4] show an Israeli main battle tank (Merkava) driving up a ramp and firing a round with a tracer over the UN 2000 Blue Line into Lebanon. After the shot it retreats from the ramp, potentially to avoid being targeted with anti-tank weapons, see Figure 7. About thirty and forty-five seconds later, distant bursts of arms fire can be heard.

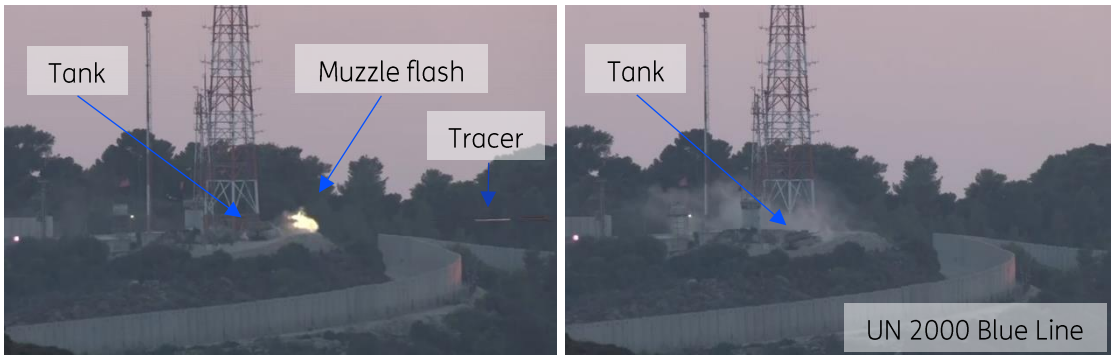

Figure 7 Reuters live feed recording, showing an Israeli tank firing from a ramp behind the UN 2000 Blue Line; the muzzle flash and round tracer are clearly visible (left). After firing the tank retreats from the ramp (right).

Roughly one minute after the main battle tank fired its round, the location of the journalists is struck by ammunition as recorded by the three cameras, which all remain in upright position. The Reuters and Al Jazeera footage do not provide a time stamp, but from the data stream (codec) of the AFP footage [AFP Footage.mp4] TNO has derived that the time of strike is 18:02:45. After fifteen seconds a woman can be heard screaming that she cannot feel her legs. After thirty-seven seconds the location of the journalists is struck again after which the Reuters and AFP cameras stop recording. The Al Jazeera camera goes down but keeps recording. Twenty-nine seconds after the second strike arms fire and bullets whizzing through the air can be heard for seven seconds. Forty-eight seconds after the second strike the woman is heard screaming that she is burning. One minute and six seconds after the second strike, arms fire and bullets whizzing through the air are heard for two seconds. After one minute and fifty-five seconds after the second strike the recording is cut, probably manually.

The course of events, as described above, is summarized in Table 1.

Table 1 Course of events.

Time	Event	Filming direction	Source
17:10	Smoke plumes behind ridge	South	AFP C6337.MP4
17:13	Smoke plumes behind ridge	South	AFP C6338 - AFP Footage to the East 1.MP4
17:14	Reparking of car	South	AFP C6338 - AFP Footage to the East 1.MP4
17:16:35	Vibration of camera probably caused by somebody touching the camera	South	AFP C6338 - AFP Footage to the East 1.MP4
17:16:38	Sound of firing of ammunition round	South	AFP C6338 - AFP Footage to the East 1.MP4
17:16:39	Sound of detonation from ammunition round	South	AFP C6338 - AFP Footage to the East 1.MP4
17:16:41	Smoke from firing and detonation of ammunition round	Southeast	AFP C6338 - AFP Footage to the East 1.MP4 ISSAM09.mp4
17:17	Smoke from detonation of ammunition round	Southeast	C6339 - AFP Footage to the East 2.MP4

17:17:20	Man says “that was outgoing”. Woman says “are we safe here?” Man says “good question”	Southeast	C6339 - AFP Footage to the East 2.MP4
17:17:35	Smoke plumes behind ridge	South	C6339 - AFP Footage to the East 2.MP4
17:17:50	Smoke plumes behind ridge, sound of sirens	South	C6339 - AFP Footage to the East 2.MP4
17:18:30 – 17:20:41	Smoke plumes behind ridge, sound of distant explosions	South	C6339 - AFP Footage to the East 2.MP4
17:34	Smoke plumes behind ridge, sound of helicopter	South	AFP C6347.MP4
17:34 – 17:38	Increasing smoke plumes behind ridge, sound of artillery fire and detonations	South	AFP C6347.MP4
17:38 – 17:40:22	Increasing smoke plumes behind ridge, sound of distant explosions and helicopter	South	AFP C6347.MP4
17:50 – 17:58:05	Smoke plumes behind ridge, sound of artillery fire and detonations	South	AFP C6351.MP4, AFP C6532.MP4, AFP C6353.MP4
18:01:45	Tank firing a round with tracer, then retreating from ramp	Southwest	Issam live footage.mp4 AFP Footage.mp4
18:02:15 – 18:02:30	Distant bursts of arms fire	Southwest	Issam live footage.mp4 AFP Footage.mp4
18:02:45	Location of journalists is hit by ammunition. All cameras remain in upright position.	Southwest	Issam live footage.mp4 AFP Footage.mp4 Al Jazeera footage. Helicopter, both strikes.mp4
18:03	Woman screams she cannot feel her legs	Southwest	Issam live footage.mp4, AFP Footage.mp4, Al Jazeera footage. Helicopter, both strikes.mp4
18:03:22	Location of journalists is hit again by ammunition. Reuters and AFP cameras stop recording. The Al Jazeera camera goes down but keeps recording.	Southwest	Issam live footage.mp4 AFP Footage.mp4 Al Jazeera footage. Helicopter, both strikes.mp4
18:03:49 – 18:03:56	Sound of arms fire and bullets whizzing through the air	Upwards	Al Jazeera footage. Helicopter, both strikes.mp4
18:04:10	Woman screams she is burning	Upwards	Al Jazeera footage. Helicopter, both strikes.mp4
18:04:28 – 18:04:30	Sound of arms fire and bullets whizzing through the air	Upwards	Al Jazeera footage. Helicopter, both strikes.mp4
18:05:17	Recording is cut, probably manually	Upwards	Al Jazeera footage. Helicopter, both strikes.mp4

Table 1 demonstrates that the journalists were present on the hilltop for at least fifty-three minutes before the incident. They were hit forty-five minutes after an ammunition round was fired and detonated to the southeast of their location. Within thirty-seven seconds they were hit a second time. Shortly after the second strike, arms fire and bullets whizzing through the air are heard. Throughout most of the recordings the sound of one or more drones is audible.

3 Firing point

The firing point used for both strikes on the journalists has been established based on the general direction of fire and triangulation using acoustics and footage, which are described in section 3.1 and 3.2 respectively. The distance to and the location of the firing point are presented in section 3.2.2. An analysis of the arms fire, audible about thirty seconds and one minute after the second strike, is presented in section 4.3.

About forty-five minutes before the journalists are struck, another strike occurred. For the purpose of completeness, the impact zone of this strike is determined at approximately 880 m to the southeast of their location based on geographical, timing, audio and video analysis. The audio of this strike is consistent with the firing of an M329 Anti-Personnel / Anti-Materiel – Multi Purpose Tank Round with Tracer (APAM-MP-T) in airburst mode from behind the UN 2000 Blue Line. An analysis of this strike is presented in Appendix A.

3.1 Direction of fire

The general direction from where the rounds were fired can be determined based on the footage at the time of the incident and on the debris pattern at the strike location. The footage and debris pattern are presented in section 3.1.1 and 3.1.2.

3.1.1 Footage

At the moment of the first strike, the Reuters, Al Jazeera and AFP cameras were pointed towards the location near the Hasulam Cave where an Israeli main battle tank fired a round one minute earlier. All recordings demonstrate a slight blur, and the rock formation on the right lights up red on the AFP footage, but none of the recordings show a muzzle flash or smoke at the Israeli position near the Hasulam Cave at the moment of the incident, see Figure 8, Figure 9 and Figure 10.

Since Kinetic Energy (KE) rounds of main battle tanks are usually fired using a muzzle velocity of 1500 to 1750 m/s, and High Explosive (HE) rounds of main battle tanks with 750 to 1000 m/s, the time of travel is at least 1 and 2 seconds respectively, over about 2 km. Since all cameras recorded at a frame rate of 25 frames per second, a muzzle flash or smoke from a round launch would have been visible on the recordings if a round was fired from that location. This demonstrates that the round in the first strike was not fired from the Israeli position near the Hasulam Cave.

Figure 8 Reuters live feed recording at the moment of the first strike [Issam live footage.mp4].

Figure 9 Al Jazeera recording at the moment of the first strike [Al Jazeera footage. Helicopter, both strikes.mp4].

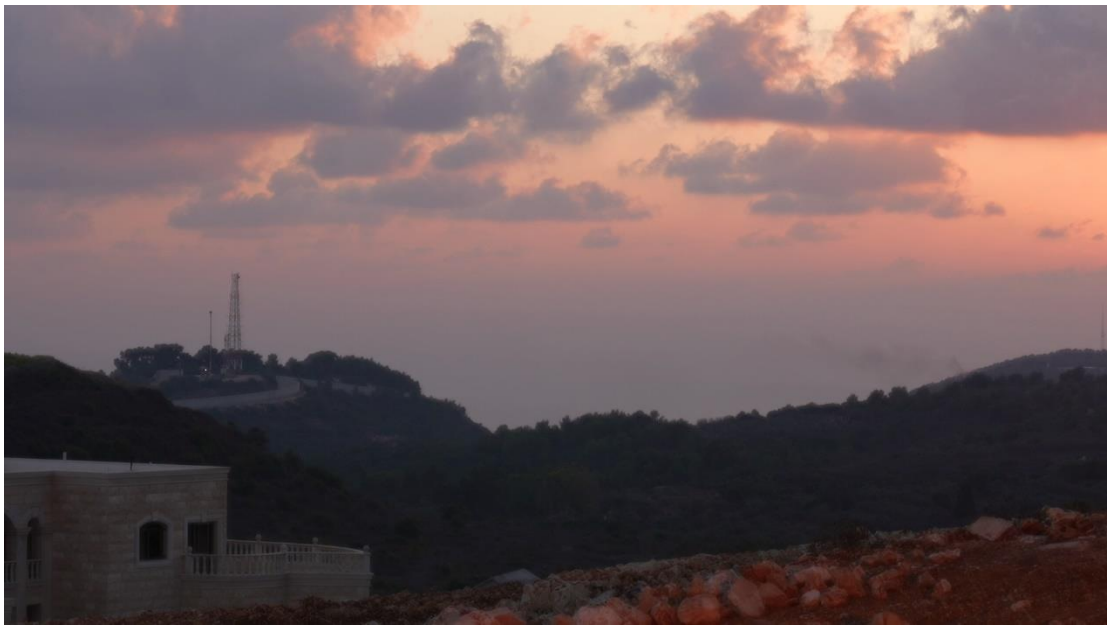

Figure 10 AFP recording at the moment of the first strike [AFP footage.mp4]. The rock formation on the right lights up red.

After the first strike, the Al Jazeera and AFP cameras remain filming the Israeli position near the Hasulam Cave and both record the second strike, see Figure 11 and Figure 12. The absence of a muzzle flash or smoke from a round launch on both recordings, demonstrates that the round in the second strike was not fired from the Israeli position near the Hasulam Cave.

Figure 11 Last frame of the Al Jazeera recording before the second strike [Al Jazeera footage. Helicopter, both strikes.mp4].

Figure 12 Last frame of the AFP recording before the second strike [AFP footage.mp4].

3.1.2 Debris pattern

A MAXAR satellite image taken on 12 October 2023, one day before the incident, shows no signs that the scene of the incident was involved in an earlier ammunition strike. This satellite image is displayed in Figure 13. Cratering, debris or burn marks are not observed at or near the incident location. This is also the case for the photograph shown in Figure 1 made by Issam Abdallah about one hour before the incident. Because there is no evidence of an earlier strike, there is no doubt that the debris observed at the scene is related to the incident on 13 October 2023.

Figure 13 MAXAR satellite image from 12 October 2023, showing no signs of an earlier ammunition strike.

The first strike hit the stone wall just north of the utility pole, leaving a substantial hole in the wall, see Figure 14. From Figure 1 it is evident that this hole was not present prior to the strike.

Figure 14 Hole in the stone wall. Clockwise: still from [Fixer - Walkthrough 1.mp4], still from [Fixer - Walkthrough 2.mp4], [IMG-20231015-WA0063.jpg] and [IMG-20231015-WA0072.jpg].

The direction of fire can be roughly aligned with the debris pattern behind the wall, which is shown in Figure 15. The debris is spread out predominantly towards the stone wall in the back of Figure 15. It is noted that the debris pattern only provides a rough indication of the direction of fire as the round may have grazed and deflected off the front of the vehicle on the other side of the road or may have impacted the wall at an angle. Grazing, deflection and a non-head on impact may result in a spread of debris not fully aligned with the trajectory of the ammunition article. An error margin of plus minus ten degrees is therefore maintained for the estimated direction of fire to account for this inaccuracy.

Figure 15 Debris field behind the wall [IMG-20231015-WA0066.jpg]. Its estimated direction is indicated.

The debris pattern is also observed on a MAXAR satellite image from 26 October 2023, see Figure 16. The image shows the hole in the wall, just north of the utility pole and the burnt wreckage of the vehicle. The white spot represents the hood of the car. The estimated direction of fire based on the debris pattern, including a ten-degree error margin, is indicated. This direction and error margin are then transferred to a Google maps image to illustrate the direction of fire plotted over a wider area. It is clear that the ammunition article that hit the stone wall was fired from the east - southeast.

Figure 16 MAXAR satellite image from 26 October 2023. The arrow represents the estimated direction of fire, with a plus minus ten-degree error margin. The white spot represents the hood of the car.

Figure 17 Estimated direction of fire based on the debris field behind the stone wall, with a plus minus ten-degree error margin [Google maps].

3.2 Triangulation

The combination of video footage, their audio tracks and the known locations of recording allows for determination of the firing point. For this exercise footage from Al Jazeera and RAI has been used. Footage of the Lebanese Broadcasting Corporation International (LBCI) is used for confirmation.

3.2.1 Acoustics and footage

The Al Jazeera footage contains the audio of both strikes at the location of the journalists. The RAI footage contains video and audio of the second strike from a viewpoint in the town of Aalma el-Chaab. The Al Jazeera, RAI and LBCI recordings are described in section 3.2.1.1, 3.2.1.2 and 3.2.1.3. Audacity software version 3.3.3 is used for analysis of the audio recordings.

3.2.1.1 Strike location

In [Al Jazeera footage. Helicopter, both strikes.mp4], the sound of both strikes can clearly be heard. Two to three seconds after the sound of each strike, a “thud”-like sound is vaguely audible. This is hypothesized to be the muzzle blast, i.e. the shockwave that occurs at the muzzle of a barrel when the round is fired. Since ammunition usually travels faster than the speed of sound, the ammunition arrives at the strike location ahead of the sound of the muzzle blast.

The audio waveform and spectrogram[4] of the time period around the first strike are shown in Figure 18. The red lines indicate the sound of impact and hypothesized muzzle blast. The impact sound can clearly be recognized in the waveform and spectrogram by the sudden spike in sound level. This is not that obvious for the muzzle blast.

[4] The spectrogram of an audio track provides a visual indication of how the energy in different frequency bands changes over time.

However, when looking at the waveform in more detail, a sudden change in amplitude and frequency can be observed, see Figure 19. The spectrogram (shown in the same figure) shows a sudden peak in low frequency sound at this point.

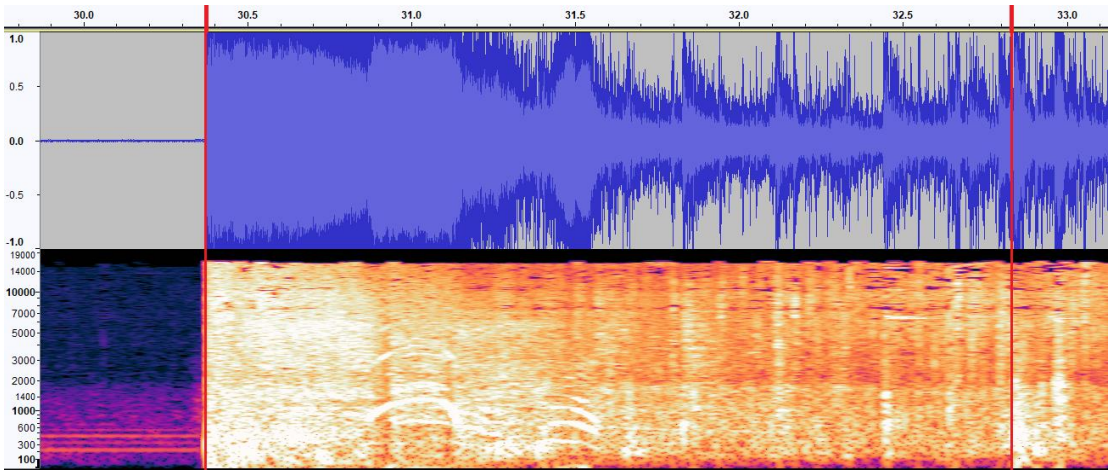

Figure 18 Audio waveform and spectrogram of the time around the first strike. The impact sound is indicated by the red line on the left, the hypothesized muzzle blast is indicated by the red line on the right.

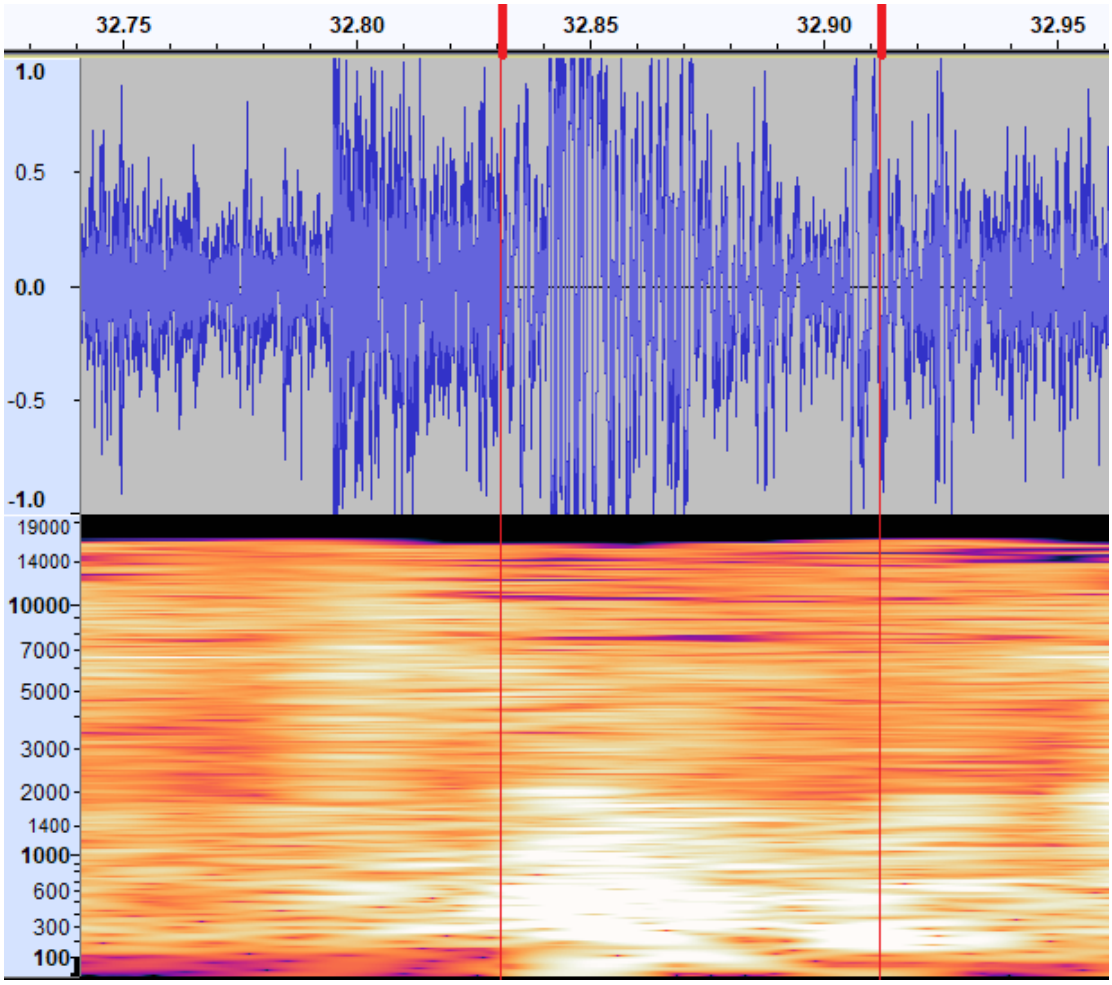

Figure 19 A detailed view of the waveform and spectrogram of the hypothesized muzzle blast after the first strike, showing a change in amplitude and frequency in between the red lines.

An identical analysis is performed for the second strike. Figure 20 and Figure 21 present the audio waveform and spectrogram of the time around the second strike and a detailed view of the waveform and spectrogram of the hypothesized muzzle blast, respectively. Comparing Figure 21 to Figure 19 shows a similar duration and change in amplitude and frequency for both muzzle blasts, as well as a similar low frequency pulse in the spectrogram. Furthermore, the interval between the sound of strike and muzzle blast is also similar for both strikes. For the first strike this interval equals 2.457 seconds, and for the second strike 2.463 seconds.

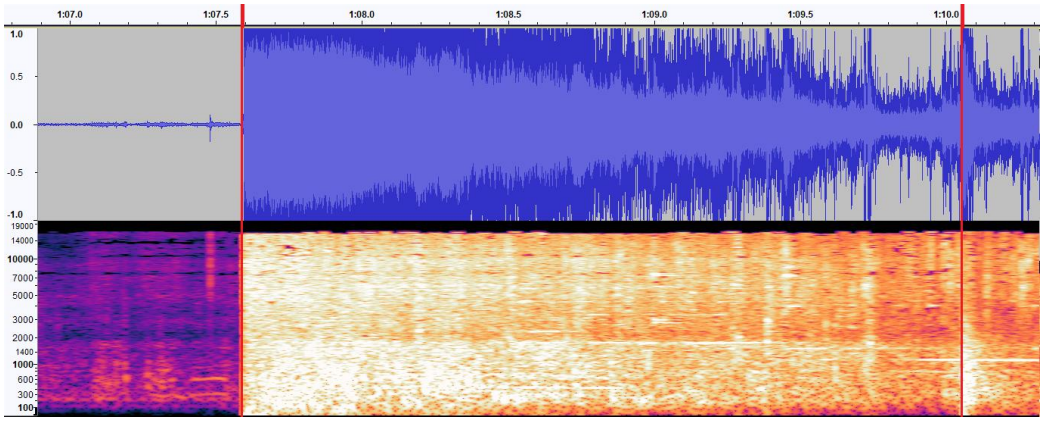

Figure 20 Audio waveform and spectrogram of the time around the second strike. The impact sound is indicated by the red line on the left, the hypothesized muzzle blast is indicated by the red line on the right.

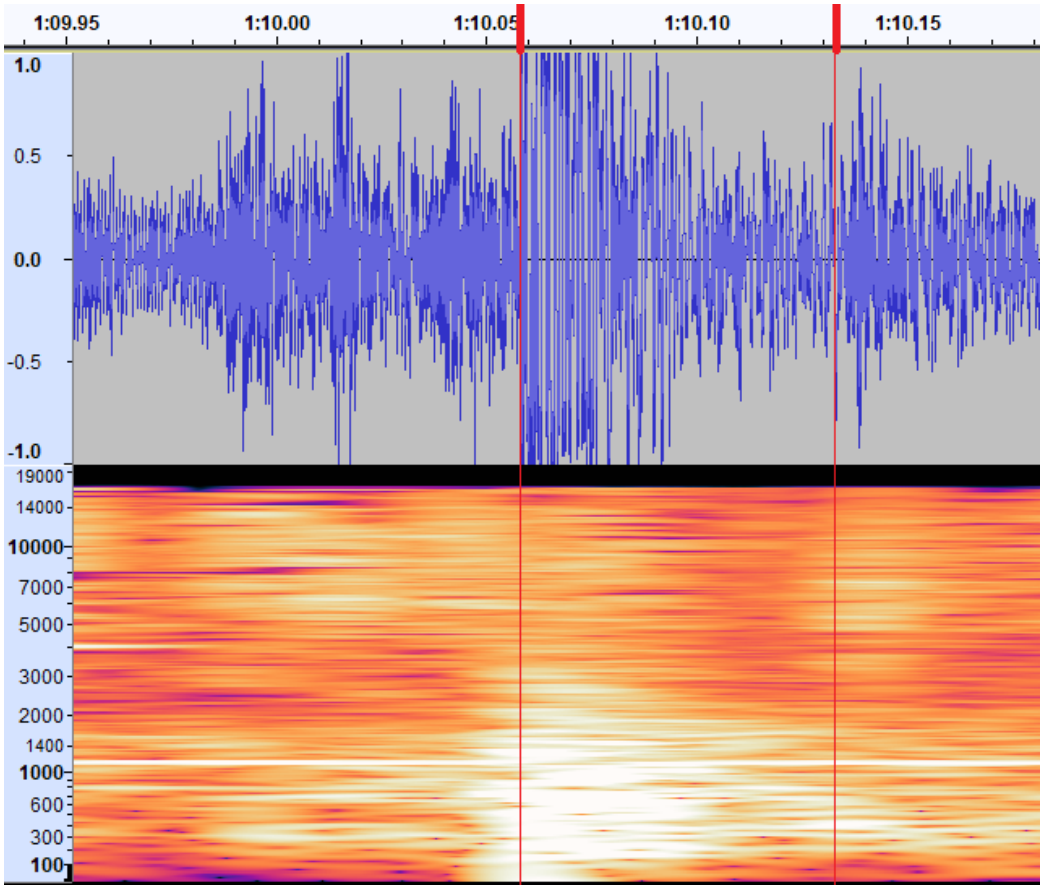

Figure 21 A detailed view of the waveform and spectrogram of the hypothesized muzzle blast of the second shot, showing a change in amplitude and frequency in between the red lines.

The fact that the change in waveform and spectrogram are similar and that the intervals are nearly identical strengthens the hypothesis that the “thud”-like sound indeed relates to the muzzle blast for both strikes.

3.2.1.2 Aalma el-Chaab

In the RAI footage [ISSAM ABDALLAH .mxf] from a viewpoint in Aalma el-Chaab, the firing and impact of the second round can be seen and heard. This footage also shows smoke and dust clouds indicative of the firing and impact of an earlier shot, see Figure 22. The sequence of events of the second shot is clockwise presented in Figure 23; a muzzle flash is seen, followed by an ammunition travelling through the air, visualized by a tracer and smoke trail, followed by a fire ball at the moment of detonation, which launches the hood and other vehicle parts into the air. The smoke and dust clouds arising from the firing and strike location prior to the second shot demonstrate that the journalists were hit twice from the same firing point.

Figure 22 Still from RAI footage [ISSAM ABDALLAH .MXF] prior to the firing of the second shot. The smoke and dust clouds reveal the firing and impact of an earlier shot.

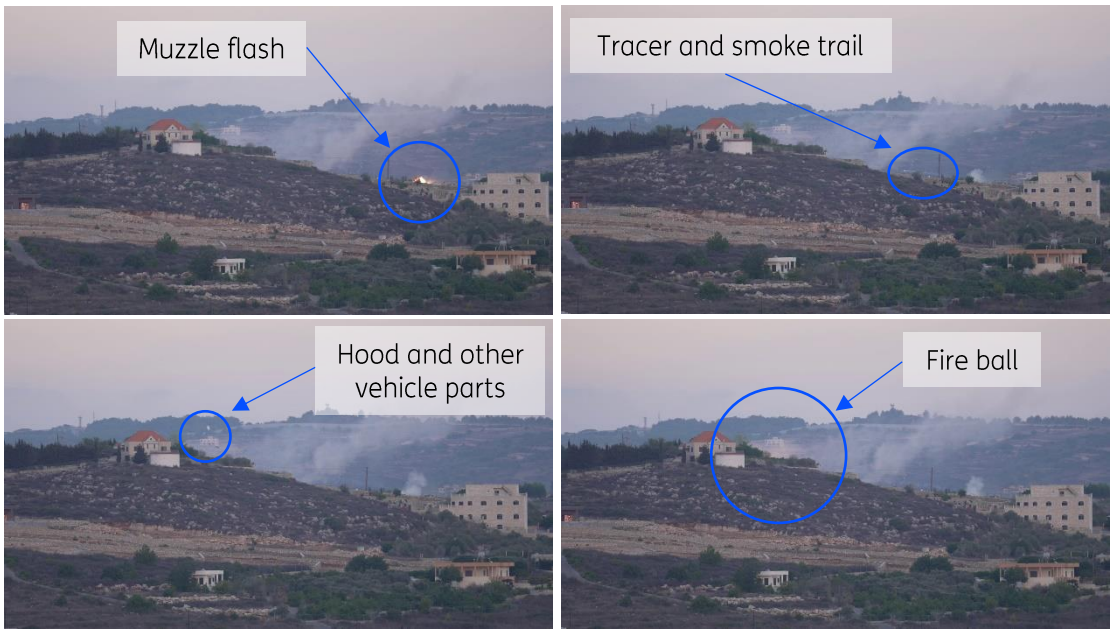

Figure 23 Stills from RAI footage [ISSAM ABDALLAH .MXF]. Muzzle flash of firing of the second round. Tracer and smoke trail of ammunition round. Fire ball lighting up the location of the journalists. Hood and other vehicle parts blown into the air (clockwise).

Figure 24 shows the waveform and spectrogram corresponding to the second shot, with red lines indicating the sound of impact (left) and the sound of firing (right). Figure 25 and Figure 26 show a detailed view of both sounds[5]. From the waveform data, it is determined that the time between seeing the firing and hearing the firing equals 8.51 seconds. And that the time between seeing the detonation and hearing the detonation is 4.54 seconds. This information can be used to calculate the distances between the firing point and the camera viewpoint, and between the strike location and the camera viewpoint, as detailed in section 3.2.2.

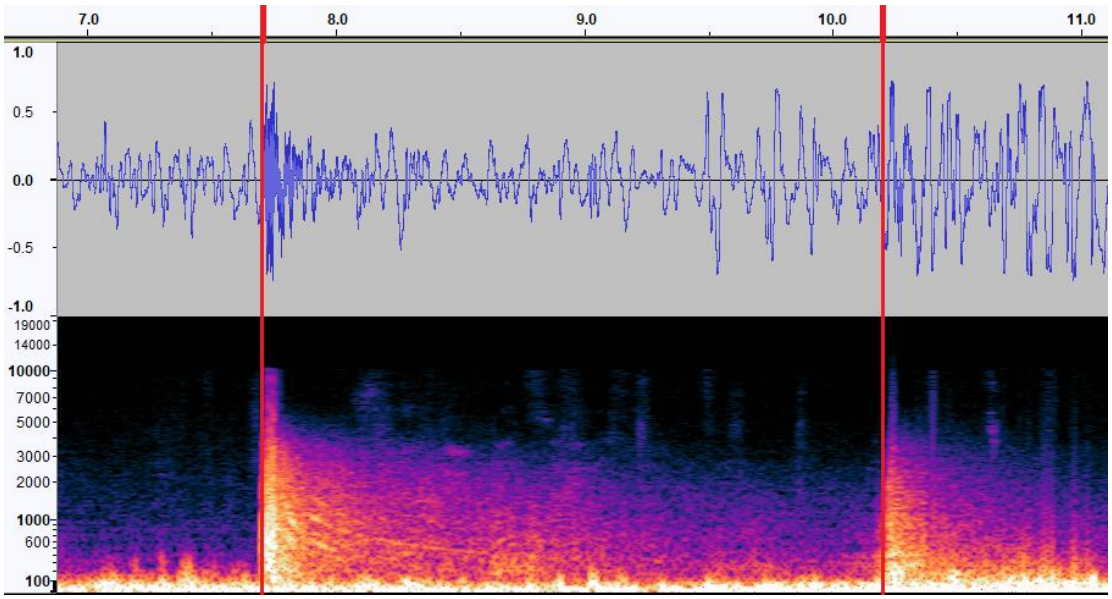

Figure 24 Audio waveform and spectrogram extracted from [ISSAM ABDALLAH .mxf] corresponding to the second shot.

[5] Duration of the sound pulse is too short to generate an accurate spectrogram for these sounds.

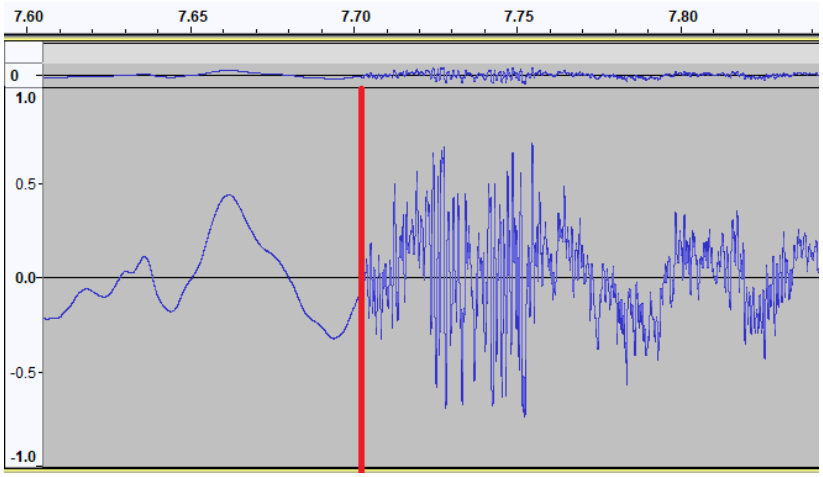

Figure 25 Audio waveform corresponding to the detonation of the second shot.

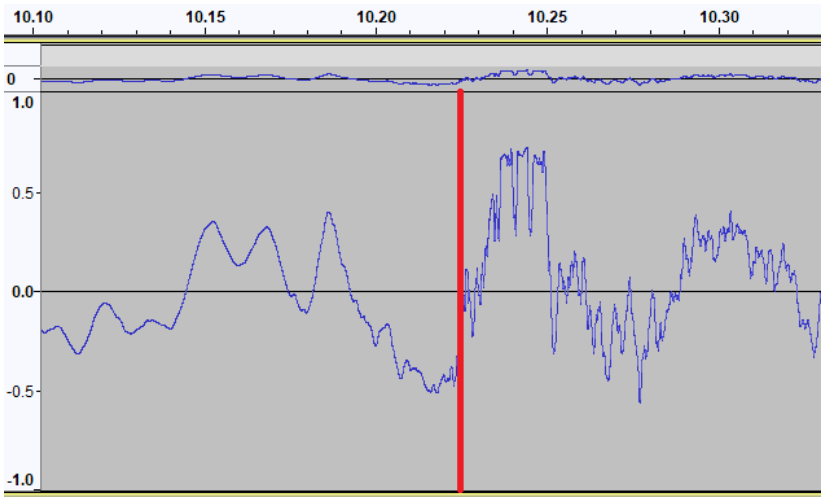

Figure 26 Audio waveform corresponding to the firing of the second shot.

3.2.1.3 LBCI filming location

Approximately 100 meters southwest of the strike location, a film crew from LBCI also captured the audio of the second strike. The audio waveform and spectrogram of this recording are shown in Figure 27. As was the case for the audio analysed in the preceding sections, both the sound of impact, as well as the muzzle blast, can be distinguished, and are indicated in the figure by red lines. Figure 28 shows a detailed view of the audio from the muzzle blast. A change in amplitude and frequency can be seen in the waveform, and a peak in low frequency sound can be seen in the spectrogram. The interval between the sound of strike and muzzle blast is 2.378 s, which is consistent with the interval determined in section 3.2.1.1.

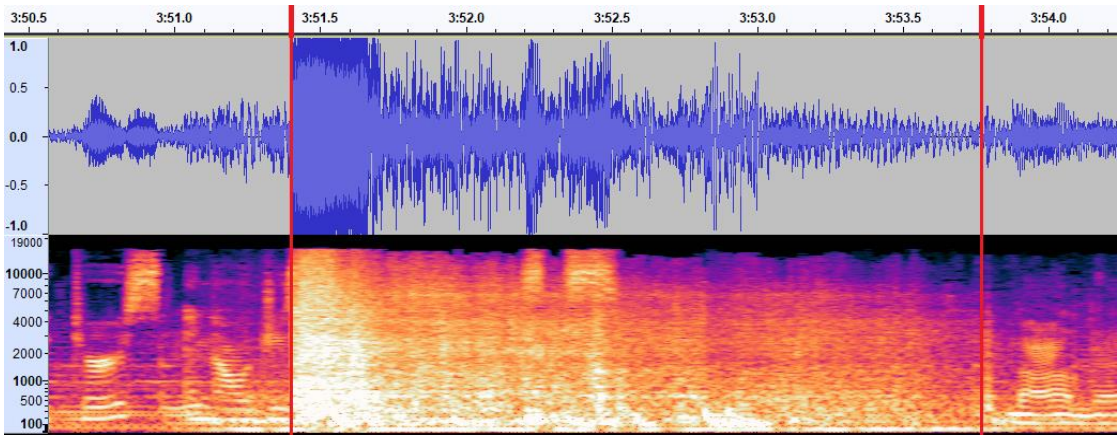

Figure 27 Audio waveform and spectrogram extracted from [YouTube: Death of Reuters reporter Issam Abdallah What happened on the Lebanese Israeli border] corresponding to the second shot.

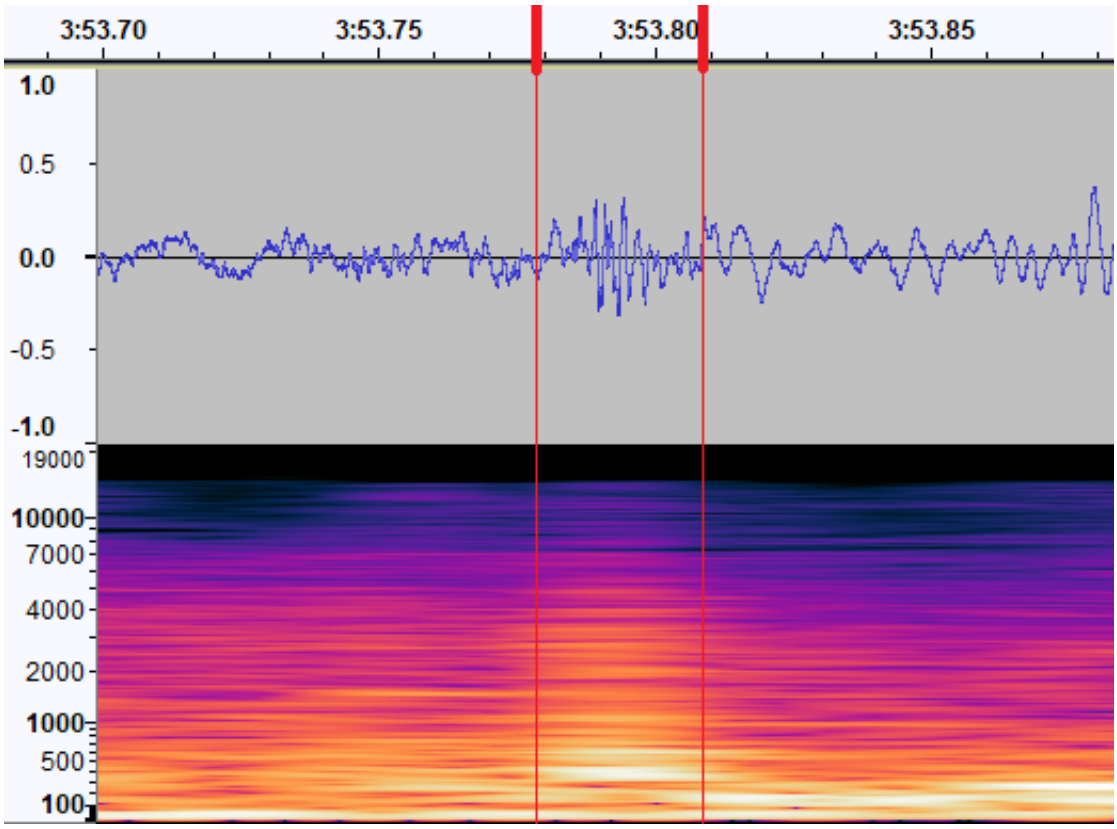

Figure 28 A detailed view of the waveform and spectrogram of the hypothesized muzzle blast of the second shot, showing a change in amplitude and frequency in between the red lines.

3.2.2 Distance and location

For the determination of the distance between firing point and strike location the following parameters are used:

- Projectile launch is at time t=0 when the projectile leaves the muzzle of the barrel with velocity $v_{pr,0}$. At the same time a blast wave radiates from the muzzle into the surrounding air, due to the momentary discharge of high-pressure propellant gaseous products;
- In flight the projectile velocity v_{pr} decreases to some extent because of air drag;
- The muzzle blast wave propagates with the sound velocity c_{air} in air;
- Projectile impact is at time t=T_0 at the strike location, which is at distance x_{impact} to the firing point. The projectile has travelled distance x at an average velocity $\bar{v}_{pr}$;
- At time t=T_1 the muzzle blast arrives at the camera viewpoint.

In [ISSAM ABDALLAH .MXF] both firing and impact of the second round are visible (see Figure 23). With 36 +/- 1 frames recorded at 25 frames per second (based on the codec), one derives T_0 = 1.44 +/- 0.04 s. In [Al Jazeera footage. Helicopter, both strikes.mp4] both the impact and muzzle blast are audible at the strike location. From sound analysis follows that (T_1-T_0) = 2.460 +/- 0.003 s (see section 3.2.1.1).

The distance x can be calculated in three ways on the basis of:

1. Projectile arrival time T_0 in combination with an assumed muzzle velocity $v_{pr,0}$;
2. The difference between blast wave and projectile arrival time (T_1-T_0) in combination with an assumed muzzle velocity $v_{pr,0}$;
3. T_0 in combination with (T_1-T_0).

The third way is chosen as no assumption regarding projectile muzzle velocity is required and thus more accurate. The derivation of x is given below:

Equation 1 $x_{impact} = \bar{v}_{pr} \cdot T_0$.

At T_0 the muzzle blast has reached a distance:

Equation 2 $x_{blast,T0} = c_{air} \cdot T_0$.

The muzzle blast needs to travel a distance $x_{impact} - x_{blast,T0}$ to be audible, i.e.:

Equation 3 $\frac{\bar{v}_{pr} \cdot T_0 - c_{air} \cdot T_0}{c_{air}} = (T_1 - T_0)$

So that:

Equation 4 $x_{impact} = c_{air} \cdot T_0 + c_{air} \cdot (T_1 - T_0)$

and

Equation 5 $\bar{v}_{pr} = c_{air} \cdot \left(1 + \frac{T_1 - T_0}{T_0}\right)$.

The first term at the right-hand side of Equation 4 is related to the visual observation of both firing and impact, and the second term to the audible observation of impact and muzzle blast at the strike location.

The local temperature reached a maximum of 27 °C on 13 October 2023 and decreased to 22 °C at about 18.00 [6]. The sound velocity c_{air} at 22 °C equals 344.3 m/s [7]. The impact distance is calculated as 1343 +/- 17 m using Equation 4. [8]

[6] Determined with https://www.ecmwf.int/en/forecasts/datasets/set-i
[7] Calculated using https://www.engineeringtoolbox.com/speed-sound-d_519.html.
[8] The variation relates to the margin in number of frames (+/-1), the interval between the sound of strike and muzzle blast (+/- 0.003 s), and temperature (+/- 1 °C).

The difference in height in the terrain within a radius of 1343 +/- 17 m is less than 40 m. This relatively small difference of height along the trajectory of the ammunition round can therefore safely be neglected in the calculation of the impact distance.
Using Equation 5 the average projectile velocity is calculated as 932 +/- 19 m/s. [8]

The distance between the RAI video location in Aalma el Chaab and the strike location is calculated based on the 4.54 s time delay between the visible and audible detonation in [ISSAM ABDALLAH .MXF], and equals 344.3 m/s * 4.54 s = 1563 +/- 11 m. In a similar way the time delay between the visible and audible firing is 8.51 s and gives a distance of 344.3 m/s * 8.51 s = 2930 +/- 13 m between the firing point and the location of the RAI camera. Three sides of a triangle are now known; the distance between firing point and strike location (1.34 km), between RAI camera and strike location (1.56 km) and between RAI camera and firing point (2.93 km). The firing point is determined by triangulation, see Figure 29. The approximated coordinates of the firing location using Google Maps are 33°05'57.3"N 35°12'44.3"E, with an accuracy of +/- 17 m. The location of the firing point is confirmed visually using landmarks in the RAI video.

Figure 29 Locations of RAI camera (left), strike location (middle) and firing point (right), in satellite and default map view [Google maps]. The total (rounded) distance of 5.84 km equals the triangle perimeter with sides 1.34, 1.56 and 2.93 km.

The firing point was at 448 m and the strike location at 429 m above sea level. There are two hills in between the two locations as shown in Figure 30. The line of sight is 10 m above the crest of the hill at 600 m from the strike location and 18 m above the crest of the hill at 1005 m.

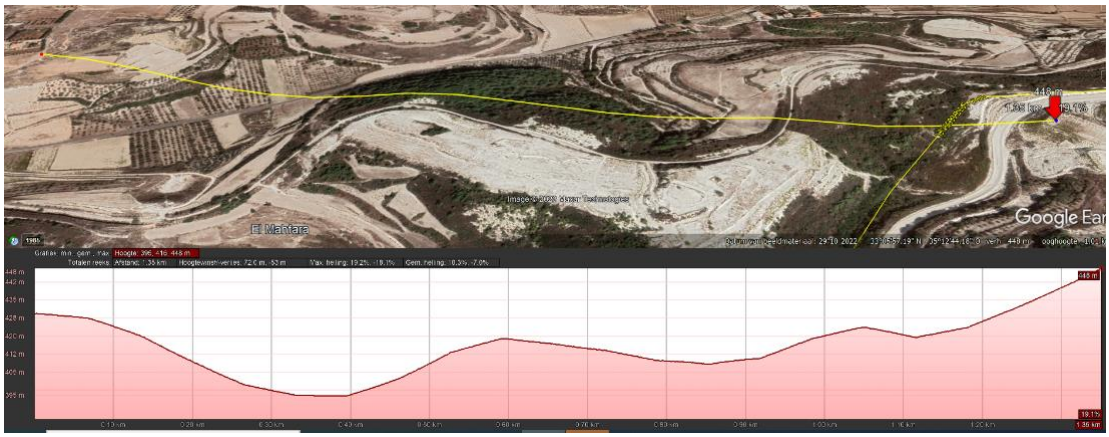

Figure 30 Profile along the line from firing point (red arrow at the right) to strike location (red dot at the left).

It can be seen that there is a line of sight between the firing point and the incident location[9]. This is also confirmed by Figure 3 and Figure 4. Figure 31 presents another still from [AFP C6338 Footage to the East 1.MP4] facing the firing point, slightly to the right of the line of sight to the radio tower.

Figure 31 Still from [AFP C6338 Footage to the East 1.MP4] facing the firing point, which is slightly to the right of the line of sight to the radio tower.

The firing location is in line with the estimated direction of fire as determined by the debris pattern (see section 3.1.2).

[9] In Figure 23, the projectile seems to come from below while the firing point is actually at a higher elevation than the strike location. Note however that the height of the strike location is obscured by a hill and that the UN 2000 Blue Line in the far distance is at 600 m above sea level. Drawing a height profile from the camera, via the strike location towards the UN 2000 Blue Line, would show that the firing point is at the same level for the RAI camera as the four storey house seen at the right of Figure 23. This means that the camera is tilted slightly upwards from the horizontal plane.

4 Ammunition and weapons

The scene of an ammunition strike is inherently complicated as it generally involves significant destruction of the impacted area and of the ammunition article itself. Analysis of a large metal piece and fragments recovered from the scene, as well as damage patterns at the scene, combined with the average projectile velocity of 932 m/s determined in section 3.2.2, provide indications for the identification of the ammunition rounds used in both strikes. Related hardware taken from the scene, such as flak vests, helmet, fragments from the Reuters car and Issam's camera, tripod and live video transmitter (LiveU) have also been investigated.

As stated in section 3.1.2, a MAXAR satellite image of 12 October 2023, one day before the incident, shows no signs that the scene of the incident was involved in an earlier ammunition strike. This is also true for a photograph made by Issam Abdallah about one hour before the incident. The MAXAR satellite image and photograph are displayed in Figure 13 and Figure 1 respectively. Accordingly, based on the available imagery, there is little doubt that the large metal piece and fragments recovered from the incident location, and the damage inflicted to the location, are all related to the incident on 13 October 2023.

The large metal piece and ammunition effects are described in section 4.1 and 4.2 respectively. The analysis of the related hardware is described in section 4.4.

4.1 Large metal piece

A large metal piece was retrieved from the site of the incident on 14 October, a day after the incident. It was found between the debris behind the stone wall with the large hole caused by the first ammunition strike (see Figure 14). The piece was situated close to the body of ISSAM Abdallah and is visible on video footage that was made moments after the incident, see Figure 32. The enlargements are marked by a blue square in the images on the left. The metal piece is indicated by blue ovals in the images on the right. Note that the observation directions of the two pictures are about ninety degrees apart. The fact that the metal piece is found behind the wall within the general direction of fire (see Figure 15), indicates that it most likely belongs to the ammunition round used in the first strike[10].

The features of the metal piece allow for identification of the ammunition round and the weapon system used for firing. These are described in section 4.1.1. Certain distinct features allow for comparison with commercially available ammunition, as detailed in section 4.1.2.

4.1.1 Identification

Examination shows that it involves a heavily damaged aluminum tail fin assembly of an ammunition. The assembly has six fixed fins, each incorporating a deployable (pop-out) fin. One of these deployable fins is still present as shown in Figure 33. Using basic workshop tools the deployable fin was dislodged from the fixed fin.

[10] The alternative, that it was part of the ammunition round that struck the vehicle, bounced off this vehicle and landed behind the wall, is considered less likely.

Because an imprint is visible on the base of the deployable fin, which matches the position of the backstop near the base of the fixed fin, it is anticipated that this fin has been deployed during flight but folded back in during impact of the round, whereas the other five deployable fins sheared off during impact. The dislodged fin, imprint and backstop are displayed in Figure 34. The fins deploy after leaving the barrel and ensure stable flight and ballistic accuracy of the round. The latter are thus not obtained by spin (rotation) of the round imparted by spiral grooves on the inside of a barrel, also referred to as rifling. The tail fin assembly allows the round to be fired with a smoothbore (unrifled) barrel.

Figure 32 Still from [IMG_9835.MOV] (top left) and Fixer - New Shell Fragment 3.jpeg (bottom left). With corresponding enlargements showing the tail fin between the debris (top and bottom right).

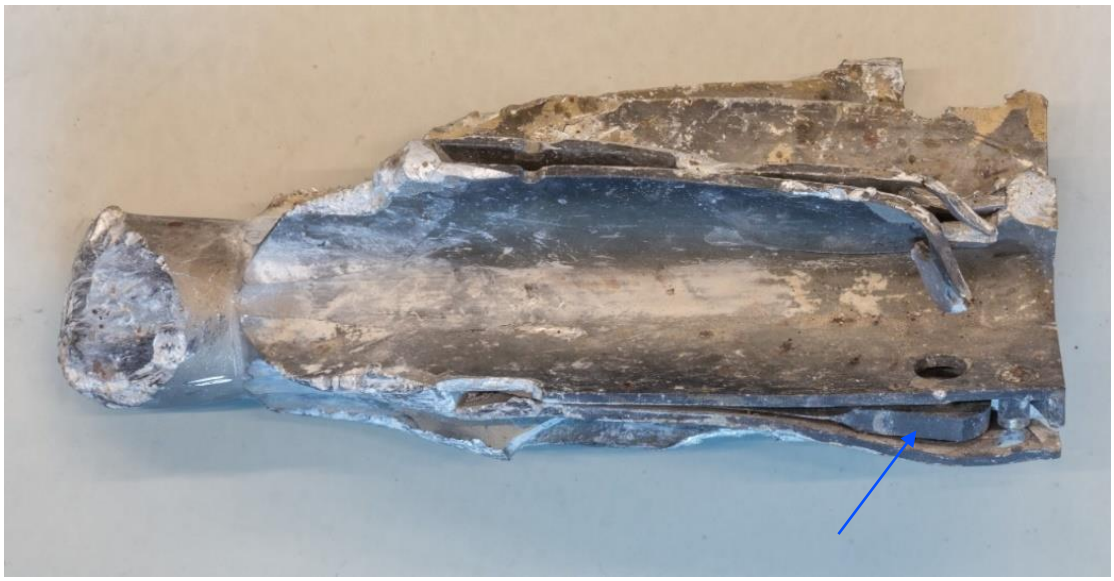

Figure 33 Aluminum tail fin assembly. One of the deployable fins is still present as indicated by a blue arrow.

Figure 34 Tail fin assembly with dislodged fin (left). An imprint is visible on the base of the deployable fin, which matches the position of the backstop near the base of the fixed fin (right).

The tail fin assembly has a base cavity with a depth of approximately three centimeters, that originally held a pyrotechnic charge, also known as a tracer, which burns during flight to enable visual tracing of the round's trajectory. The use of an ammunition round with a tracer is confirmed for the second strike by the RAI footage (see top right image in Figure 23). Lab analysis by means of energy dispersive X-ray (EDX) using a scanning electron microscope (SEM), revealed strontium and magnesium in this pocket which are typical compounds of a tracer composition. The distance between the center of the pocket and the tip of an intact fixed fin measures approximately 60 mm, as demonstrated in Figure 35. The diameter of the fin assembly accordingly approximates 120 mm, matching the inside diameter of a 120 mm cartridge.

Figure 35 The distance between the center of the pocket and the tip of an intact fixed fin measures 60 mm.

Comparable tail fins are used in mortar bombs, but these are attached to a relatively small diameter hollow shaft, or flame tube, which holds a primary ignition cartridge and external propellant charge increments that are ignited through small holes in the shaft. Since the retrieved tail fin assembly has no flame tube it is not related to a mortar bomb. Therefore, the possibility of a mortar bomb strike is ruled out.

Based on its features, the large metal piece recovered from the incident scene is identified as a tail fin assembly of a 120 mm tank round (cartridge) with a tracer, that was fired using a 120 mm smoothbore gun of a main battle tank.

Further identification was attempted based on a small marking on the tail fin retrieved from the scene. This marking was discovered near the top of the shaft close to where it originally was attached to the warhead. As shown in Figure 36, the marking appears to represent an encircled “19”. This marker may refer to the tail fin manufacturer, but this could not be confirmed.

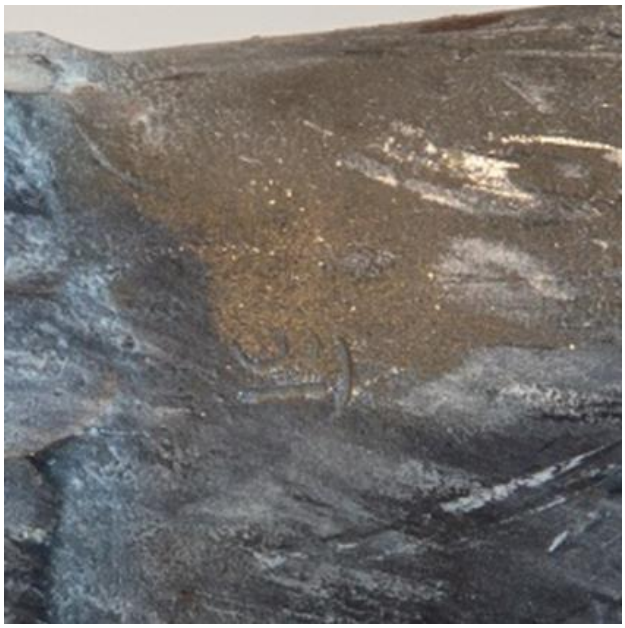

Figure 36 Marking on the tail fin shaft, possibly representing an encircled “19”.

For chemical (explosive) trace analysis, the tail fin was sampled by swabbing its surface with a sterile cotton swab soaked in 50%/50% methanol/acetonitrile (MeOH/CAN). The same has been done in and around the tracer pocket. A blank is taken by repeating the process of soaking, without wiping over a surface. The cotton swabs were placed in a gas chromatograph (GC) vial containing 50%/50% MeOH/ACN. An extraction time of about 120 minutes was maintained. The liquids were filtered with a 0.45 µm polytetrafluorethylene (PTFE) filter, with the first drops being rejected. The samples were analyzed with a gas chromatograph mass spectrometer (GCMS)[11]. The results of the analysis are shown in Figure 37. No difference is observed between the swabs of the tail fin, tracer pocket and blank.

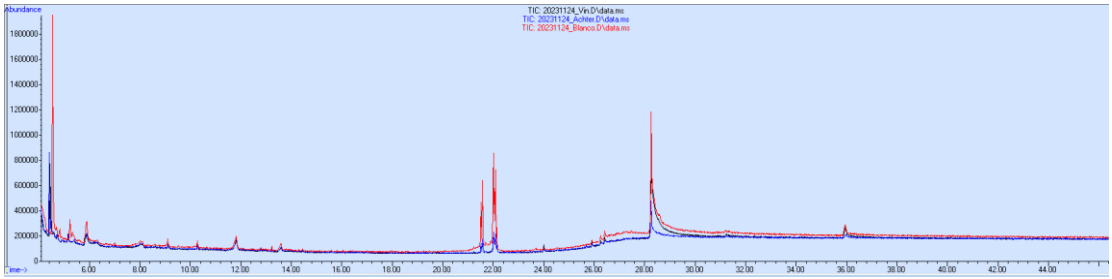

Figure 37 GCMS analysis results.

Subsequent sampling was performed of the GCMS headspace using a carboxin/divinylbenzene/polydimethylsiloxane solid phase microextraction (CAR/DVB/PDMS SPME) fiber. This was done to investigate whether any explosive residue was present in the headspace. The SPME fibers were processed in duplicate by first taking a blank of the fiber and then sampling for an hour in the bag containing the tail piece. No trace of high explosive material (like RDX) was found.

Traces of explosive were not found by sampling of the surface of the tail fin. Explosive traces, if any, may have burnt or evaporated completely.

[11] The GC is an Agilent 7890B with an Agilent HP-5MS column with a dimension of 30m, 0.25 mm and a film thickness of 0.25 µm. The MS is an Agilent 5977B MS detector.

4.1.2 Comparison to available ammunition

120 mm caliber tank rounds are produced all over the world. Certain distinct features of the tail fin assembly retrieved from the incident location are similar to those of the 120 mm Hatzav cartridge, developed by Israel Military Industries (IMI) Systems. Figure 38 displays this cartridge with a cut-out, showing its tail fin.

Figure 38 The 120 mm tank round Hatzav [Wikimedia Commons, 2015].

Close examination of details in the design of the tailfin reveals that the tail fin retrieved from the incident scene closely resembles the tail fin of the 120 mm Hatzav. The side-by-side comparison in Figure 39 demonstrates the following similar distinct features, from base to top:

- Base cavity to house the tracer;
- Pin near the base of each fixed fin, serving as backstop for the deployable fin;
- Position of the hinge in each of the fixed fins for rotation of the deployable fin;
- Position of the notch[12] on the edge of each fixed fin.

[12] Through the notches runs a cord to keep the deployable fins in place. This cord is burnt away by the propellant allowing the deployable fins to rotate when the cartridge leaves the gun barrel upon firing.

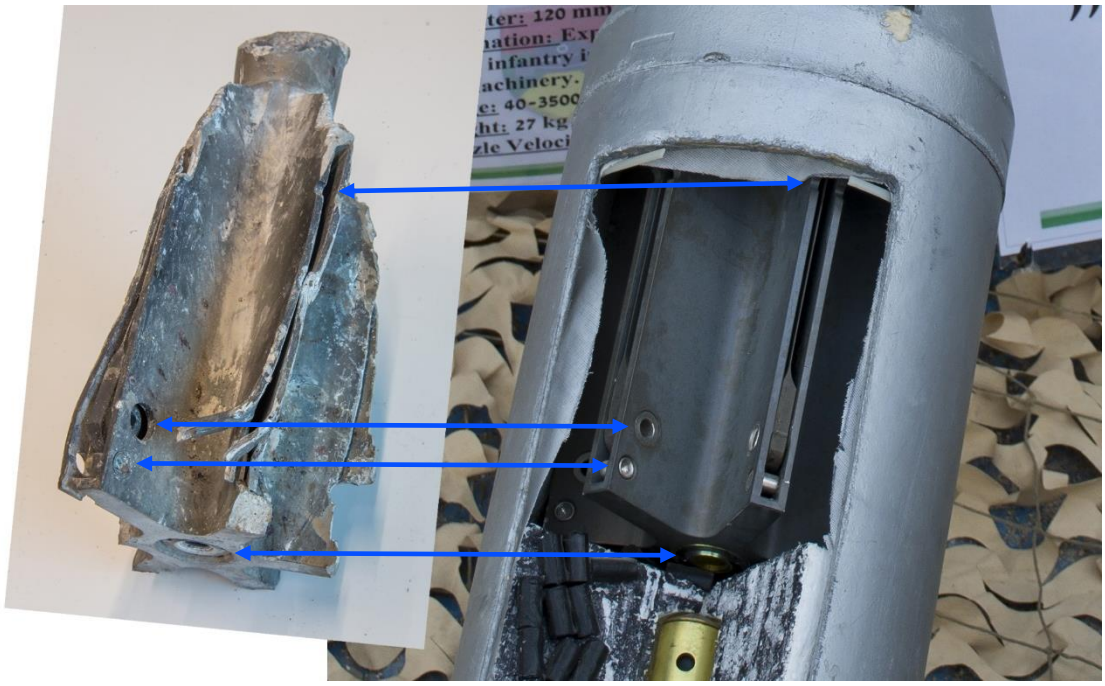

Figure 39 Side-by-side comparison of the tail fin retrieved from the incident scene (left) and the tail fin of the 120 mm Hatzav round (right). Similar distinct features are indicated by blue arrows.

The Hatzav tank round is also known as the M339 High Explosive Multi-Purpose Tracer tank cartridge with tracer (HE-MP-T), produced by Elbit Systems Land[13], see [YouTube, 2017] and [Elbit Systems, 2023]. The M339 is used by the Israeli armed forces and has been exported to Finland, Sweden, Spain and Italy. Two other rounds with a similar tail fin assembly that are produced by Elbit Systems Land include the M325 High-Explosive Anti-Tank Multi-Purpose cartridge with tracer (HEAT-MP-T) and the M329 Anti-Personnel / Anti-Materiel – Multi Purpose Tank Round with Tracer (APAM-MP-T). The latter is shown in Figure 40. All three rounds use the same tail fin assembly. Note the resemblance of the deployed fins with the one shown in Figure 34.

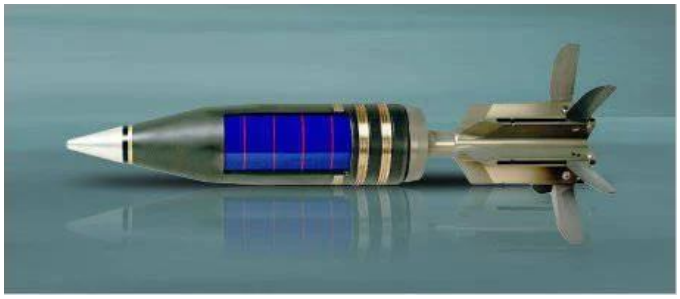

Figure 40 APAM-MP-T with tail fin assembly [Military Review, 2015].

The tail fin assembly of alternative rounds such as the M322 and M338 Armor-Piercing, Fin-Stabilized Discarding-Sabot Tracer tank cartridge (APFSDS-T) does not bear a resemblance to the tail fin retrieved from the incident scene. This is also true for an alternative 120 mm Insensitive Munition (IM) HE-T round produced by General Dynamics Ordnance and Tactical Systems (GDOTS) / NAMMO, for a 120 mm Nexter multimode HE round and Rheinmetall DM11 MP-HE-T. All three are missing the pin near the base of each fixed fin, serving as backstop for the deployable fin, see Figure 41.

[13] In 2018 Elbit completed acquisition of IMI.

Figure 41 120 mm HE rounds with cut-outs: GDOTS / NAMMO [GDOTS, 2023] (left) and Nexter [FOB, 2023] (middle), and Rheinmetall DM11 MP-HE-T [Rheinmetall, 2023] (right).

The M322 and M338 APFSDS-T, M325 HEAT-MP-T and M339 HE-MP-T are presented in the Elbit Systems Land Tank Ammunition Portfolio [Elbit Systems, 2023], which states that the 120 mm series is certified for 120 mm NATO smoothbore guns used by Merkava tanks 3 and 4 and approved for firing from NATO 120mm smoothbore gun systems L44/L55. Information on the M329 APAM-MP-T and M339 HE-MP-T is presented in [Schirding, 2007] and [Moav, 2008]. Technical specifications and performance details are summarized in Table 2.

Table 2 Specifications of Elbit 120 mm tank ammunition fired with smoothbore L44 or NATO gun barrel.

Type	Purpose	Explosive	Fuze	Muzzle velocity [m/s] at +21°C
M322 APFSDS-T	Tungsten alloy penetrator against armour	none	None	1705
M338 APFSDS-T	Tungsten alloy penetrator against armour	none	None	1680
M325 HEAT-MP-T	Shaped charge against MAVs and LAVs and fragmentation against infantry in the open	1.8 kg Comp. B	Electric PIBD	1078
M339 HE-MP-T	Against bunkers, field fortification and urban structures, LAVs and APC with medium protection armour and dismounted infantry. Capable of penetrating 200 mm double reinforced concrete walls	2.3 kg CLX663 (IM)	Electronic programmable AB, PD, PDD Grazing function	900
M329 APAM-MP-T	Against infantry, LAVs and helicopters, penetrate bunkers and buildings, breach walls	unknown	Electronic programmable Unitary AB, PD, PDD, Ejection of 6 warheads (AB) Grazing function, AB as backup to ejection mode	900 or 930

MAVs = Medium Armoured Vehicles, LAVs = Light Armoured Vehicles, APC = Armoured Personnel Carrier, Comp. B = Composition B (TNT/RDX), CLX663 (RDX/Aluminum/Wax), IM = Insensitive Munition, PIBD = Point Initiating Base Detonating, AB = Airburst, PD = Point detonating, PDD = Point Detonating Delay.

Figure 42 presents a line-up of the aforementioned tank rounds, showing the resembling tail fin assemblies for the M325 HEAT-MP-T, M339 HE-MP-T and M329 APAM-MP-T, but not for the M322 APFSDS-T.

Figure 42 Line-up of Israeli Merkava 120 mm rounds, from left to right: M322 APFSDS-T, M325 HEAT-MP-T, M339 HE-MP-T and M329 APAM-MP-T [X, 2023, 1].

Given their purpose, their different tail fin design and their relatively high muzzle velocity compared to the calculated average projectile velocity of 932 +/- 19 m/s for both rounds (see section 3.2.2), the M322 APFSDS-T and M338 APFSDS-T are ruled out to have been used in the incident. The use of one or two M325 HEAT-MP-T rounds is considered unlikely because of their purpose and muzzle velocity of 1078 m/s, which is also well above the calculated average projectile velocity. Because of their purpose and muzzle velocity that is comparable to the calculated average projectile velocity, it is anticipated that two M339 HE-MP-T rounds, two M329 APAM-MP-T rounds or a combination of both rounds have been fired in the strikes.

4.2 Tank ammunition effects

The M339 HE-MP-T and M329 APAM-MP-T rounds have multiple effect modes regulated by their fuze settings, see Table 2. These modes are described in sections 4.2.1, 4.2.2 and 4.2.3. The effects are then compared to the actual consequences for strike one and two in sections 4.2.4 and 4.2.5 respectively.

4.2.1 Airburst

Tank rounds can be fired overhead to incapacitate personnel. In airburst mode the M339 HE projects fragments from the mortar bomb warhead casing mainly radially, and fragmentation balls to the front conically (see Figure 42). The M329 APAM projects fragments in a unitary fashion or by six warheads separately after ejection from the projectile in flight, as illustrated in Figure 43. The unitary airburst mode serves as a backup when the ejection mode fails to function [Schirding, 2007]. Figure 44 shows fragments hitting the ground from an M339 detonating in airburst mode. The tail fin, encircled in blue, continues travelling along the flight path.

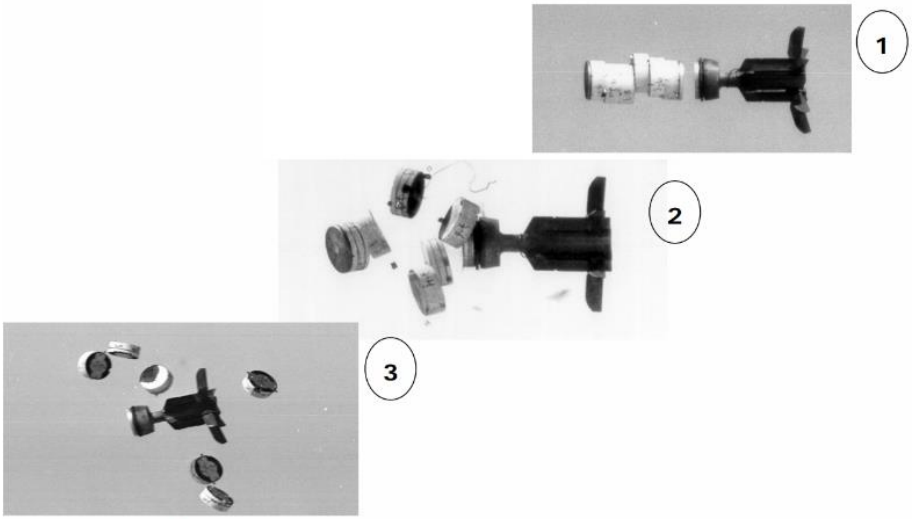

Figure 43 Warhead separation and radial dispersion of M329 APAM in airburst mode [Schirding, 2007].

Figure 44 Airburst of a M339 HE-T rank round. The tail fin is encircled in blue [YouTube, 2017].

4.2.2 Point Detonation

Examples of the effects of an M329 APAM or M339 HE in PD (super quick) mode could not be found. Figure 45 illustrates the effects of a 120 mm MP-HE-T round of an M1A1 Abrams tank when striking a concrete wall. Typically a structure is demolished, or a wall of the structure is breached with a hole (far) exceeding the diameter of the round. In Figure 46 the breaching of a 120 mm HE-MP-T striking a double reinforced concrete wall is demonstrated. Though most of the displaced wall material is flying in the forward direction of the projectile, some debris from the impact plane is projected backwards. In Figure 47 the same round strikes a truck. The observed fireball encompasses the truck on all sides. In the latter figure, the tail fin is continuing to travel along its flightpath.

Figure 45 120 mm MP-HE-T round of an M1A1 Abrams tank striking a concrete wall from right to left in PD mode [YouTube, 2016].

Figure 46 Northrop Grumman 120 mm MP-HE-T XM1147 Advanced Multi-Purpose (AMP) round striking a double reinforced wall from left to right in PD mode [YouTube 1, 2019].

M1147 Advanced Multi-Purpose Round (AMP)

Figure 47 Northrop Grumman 120 mm MP-HE-T XM1147 Advanced Multi-Purpose (AMP) round striking a truck (at the driver's door) from left to right in PD mode [YouTube 2, 2019].

4.2.3 Point Detonation Delay

In point detonation delay mode the round detonates with a delay, i.e., after the projectile has perforated the target with a hole (slightly) overmatching the 120 mm diameter of the round. An example of the effects is presented in Figure 48.

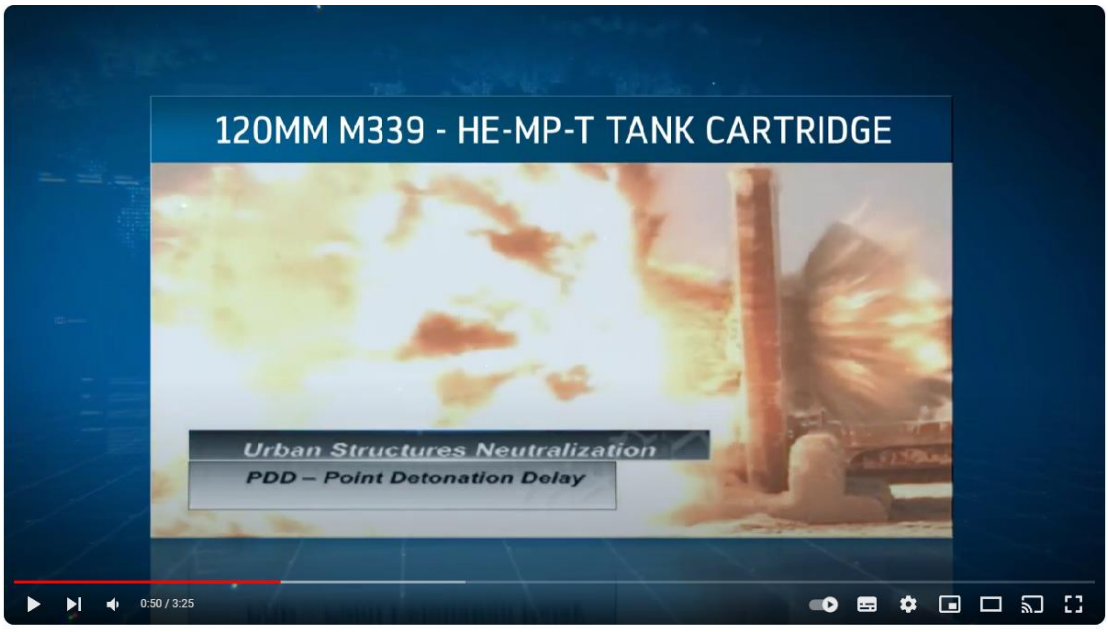

Hatzav 120mm M339 HE MP T Tank Cartridge

Figure 48 M339 HE-T rank round striking a wall from the right PDD mode and detonation observed at the left after penetration of the wall [YouTube, 2017].

4.2.4 First strike

Based on the available video recordings and photographs taken it is anticipated that Issam Abdallah was instantly killed by a direct hit severing his legs from his body. The round struck a hole in the stone wall as shown in Figure 14 and Figure 15. The exact nature of the first strike however remains subject to conjecture. As the round breached the wall, functioning of the round in airburst mode seems unlikely. For a scenario where the white car was targeted and nearly missed, a PD instead of PDD mode, seems the most likely fuze setting. Possibly, a strike with effects similar to Figure 45 and Figure 46 may have occurred. The major injuries to Christina Assi's legs may have been caused by debris coming of the wall, or by fragments of the shell. Failure of the round to detonate is considered less likely as the RAI crew pointed their camera to the sound of the strike and the finding of chunks of explosive and parts of the round other than the tail fin, has not been reported. As both types serve a similar purpose, it is anticipated that the first round was a M329 APAM-MP-T or a M339 HE-MP-T, with a fuze in PD mode.

4.2.5 Second strike

As it is anticipated that the first round missed the white vehicle, it is considered likely that the second strike was again aimed at it. For this strike there is clear evidence that a high explosive round detonated on the left front wheel or fender or entered the engine compartment of the vehicle parked next to the road (see Figure 1). A crater is formed in the asphalt and the car and the surrounding vegetation are set on fire possibly by hot fragments from the warhead or from the vehicle. Due to the blast pressure the car is displaced on to the asphalt and has rotated nearly ninety degrees from the original position, see Figure 49. Possibly, a strike with effects as shown in Figure 47 has occurred.

Figure 49 Still from [IMG_9833.MOV]; burning car, crater and vegetation due to the second strike.

The following observations are made, see Figure 50 and Figure 51. General vehicle damage:
1. Vehicle severely burned after the strike;
2. Left rear wheel seems to be melted by the heat as melted aluminum is seen on the ground surface;
3. Lot of debris around vehicle, mostly plastic parts.

Blast damages:

- Structural deformations are seen of firewall (bulkhead), bonnet stiffeners, stiffener top part of left front fender, left front door;
- Bonnet cover plate launched over the wall;
- Left fender launched, probably near wall;
- Left front wheel launched, probably completely broken as four wheel bolts are still in hub;
- Left front wheel brake disc broken, part seen at short distance from vehicle;
- Damages to parts around the engine, exhaust manifold and brake booster destroyed;
- Left chassis beam and wheel suspension intact, but damaged;
- Left doors probably opened by the blast and resulting motion of the vehicle.

Fragment damages:

- Perforations by fragments seen in stiffener left fender, bonnet stiffeners (left side), firewall, left front door, left chassis beam;
- Perforations are a mix of small circular/oval holes and bigger holes typical for natural formed fragments;
- Circular pattern of holes seen in line of the fire wall, left side bonnet, stiffener left fender.

Figure 50 Deformation and fragment punctures of the metal car body [Fixer – Car Hood 3.jpg].

The above listed observations are typical consequences of a detonating high explosive fragmenting ammunition round. Near the edge of the crater a metal fragment and a deployable fin from a tail fin assembly are observed, see Figure 51.

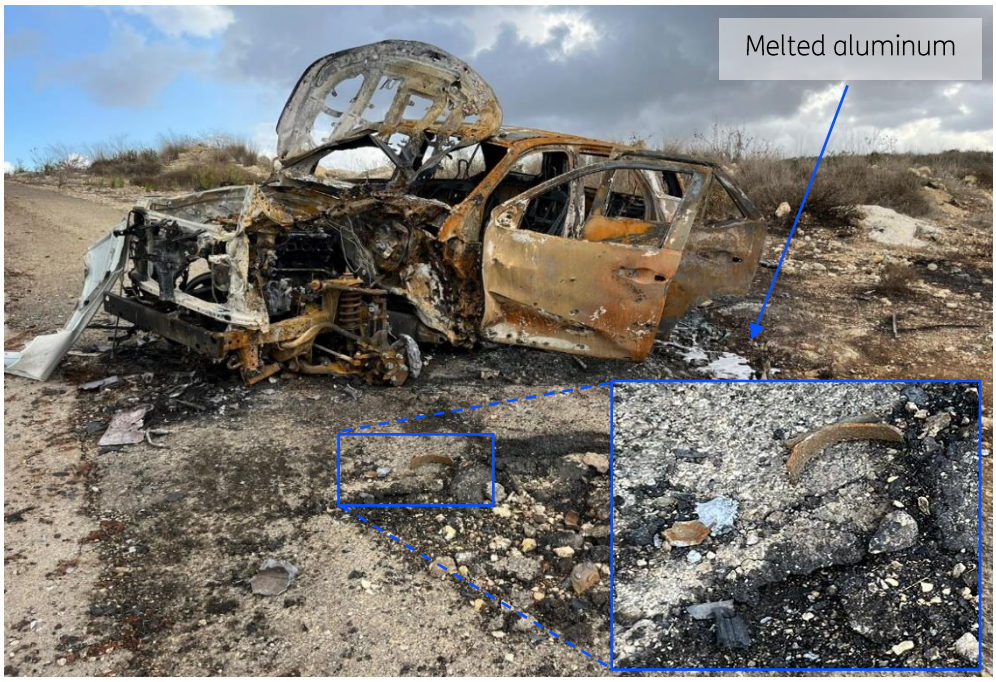

Figure 51 Near the edge of the crater a metal fragment and a deployable fin are observed [IMG-20231015-WA0074.jpg], [IMG-20231015-WA0079.jpg (cropped)]. The left rear wheel seems to be melted.

The metal fragment, shown in Figure 52, is a typical fragment from a thick cased ammunition round. Given its location, it is thought to relate to the second strike. The thickness of the fragment flat surface measures 4.5 mm. At the raised edge, seen in the top image of Figure 52, the thickness equals 5.0 mm. Using SEM-EDX, it was determined that the fragment is made of silicon steel[14] with an aluminium piece attached to it. The latter may have flown on top of it coming from a car rim that was melting when the vehicle was burning after the strike.

Figure 52 Fragment from thick cased ammunition round with molten aluminum attached [M5.jpg], [M1.jpg].

[14] With elements in weight %: C (2.5), Mg (<0.1), Al (0.1), Si (3.3), S (<0.1), Ca (<0.1), Cr (<0.1), Mn (0.8), Fe (93.0).

The fragment was compared against the casing design of the M329 APAM-MP-T and M339 HE-MP-T (see Figure 42) but the analysis remains inconclusive. As both rounds serve a similar purpose and combine a high explosive warhead with fragmentation, it is anticipated the second round has likely been a M329 APAM-MP-T or a M339 HE-MP-T, with a fuze in PD mode.

4.3 Arms fire

The Reuters and AFP cameras stop recording at the moment of the second strike. The Al Jazeera camera goes down but keeps recording. About thirty seconds and one minute after the second strike, arms fire can be heard [Al Jazeera footage. Helicopter, both strikes.mp4]. The moments of the strikes and arms fire are shown in Figure 53. The arms fire consists of one burst of about 25 shots, followed by two bursts of about nine and twelve shots (Figure 54), one burst of three shots (Figure 55) and a single shot (Figure 56).

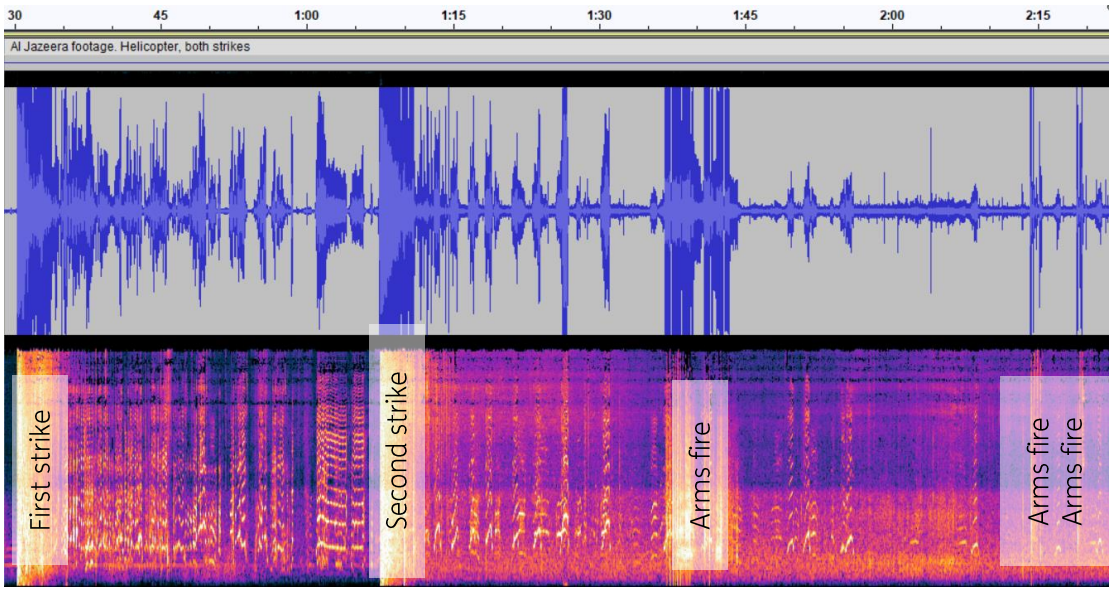

Figure 53 Waveform and spectrogram with the moments of the first strike, second strike and arms fire.

The bullets travel at supersonic speed creating a shockwave resulting in a sonic boom. This is a continuous effect until the bullets, slowed down by air drag, pass the sound barrier to subsonic speeds. The shockwave angle becomes less pointed with decreasing bullet velocity. When the sonic boom reaches the microphone of the camera a loud crack-type of sound is heard. This crack reflects off surrounding surfaces resulting in a tail of the waveform. Later in time the muzzle blast, which travels at sonic speed, reaches the camera. The exact number of shots in Figure 54 is hard to determine as the sonic boom of the last bullets in the burst overlap with the muzzle blasts of the first bullets.

The audio for the burst of three shots in Figure 55 allows for determination of the interval between the sonic boom and muzzle blast per shot. These intervals are 0.97 s, 0.97 s and 0.90 s for shot number one, two and three respectively[15]. In between the sonic booms and muzzle blasts, two whiz-type of sounds are heard that are thought to represent bullets that are travelling at subsonic speed at close range to the microphone. The interval between the sonic boom and bullet whiz of the third shot can be distinguished. This interval starts at about 0.313 s and ends at about 0.428 s, and measures roughly 0.35 s where the whiz has the highest amplitude.

[15] Differences may result from the alternate use of ball, armour piercing and tracer cartridges in the ammunition belt.

The audio for the single shot in Figure 56 includes a tick and metallic sound that is thought to relate to an impact. When the sonic boom is set at t = 0 s, the reflection occurs at 0.026 s[16], the bullet whiz at 0.25 s (at the highest amplitude), the metallic impact sound at 0.49 s and the muzzle blast at 0.89 s.

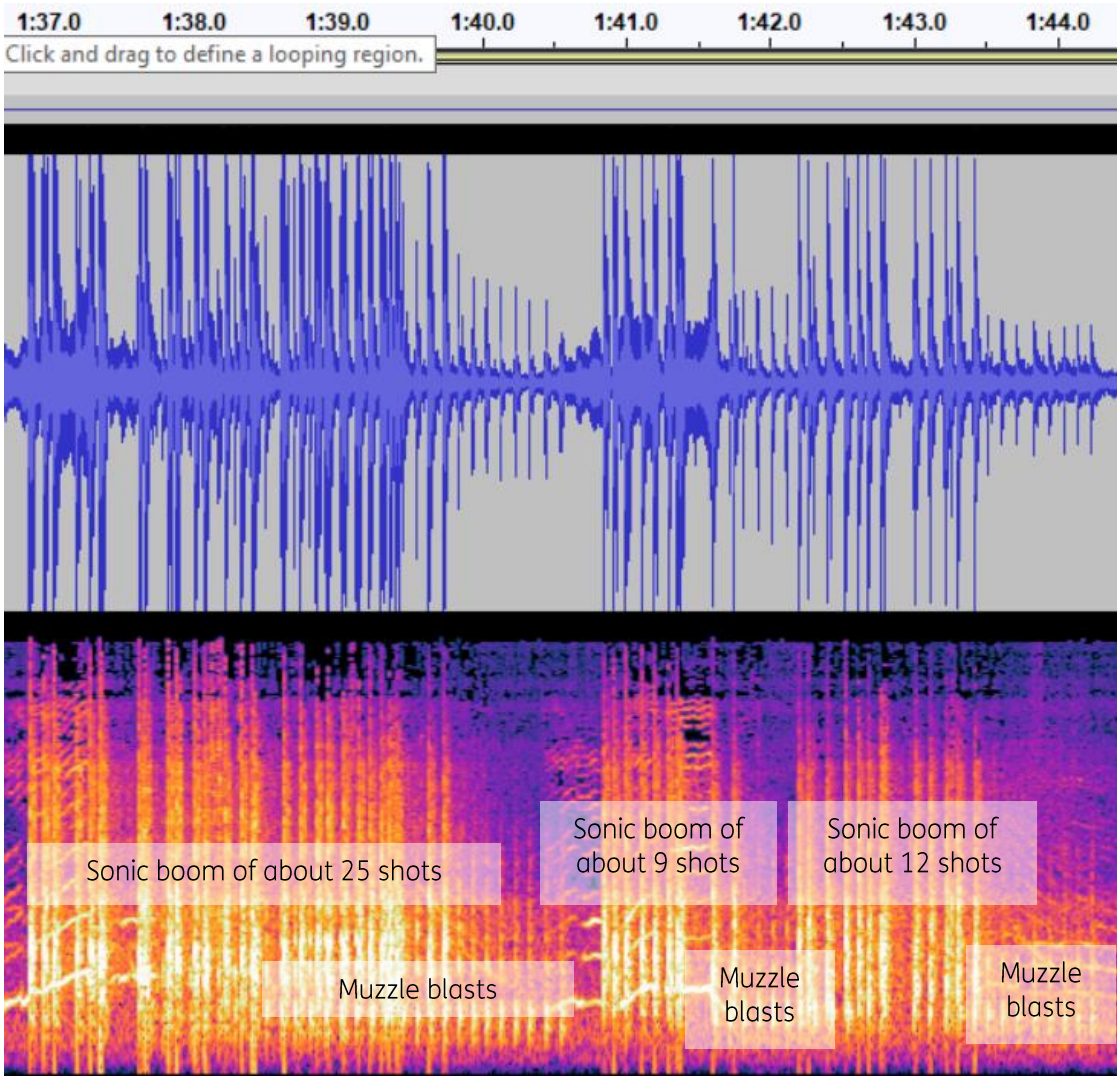

Figure 54 Three bursts of arms fire: sonic boom of about 25 shots, followed by the sonic boom of about nine shots and of about twelve shots.

The bursts in Figure 54 are compared against measurements made by TNO of .50 caliber (12.7 mm) rounds fired by a heavy machine gun on a firing range of the Netherlands Ministry of Defence (MoD). The frequency of the highest sound exposure levels of the sonic booms of around 1000 Hz, and a lower spectrum for the muzzle blasts, are found to be consistent with the TNO measurements.

[16] It may also be a different propagation path through the atmosphere. So in that case the whole signal is the tail. Including interactions with the ground.

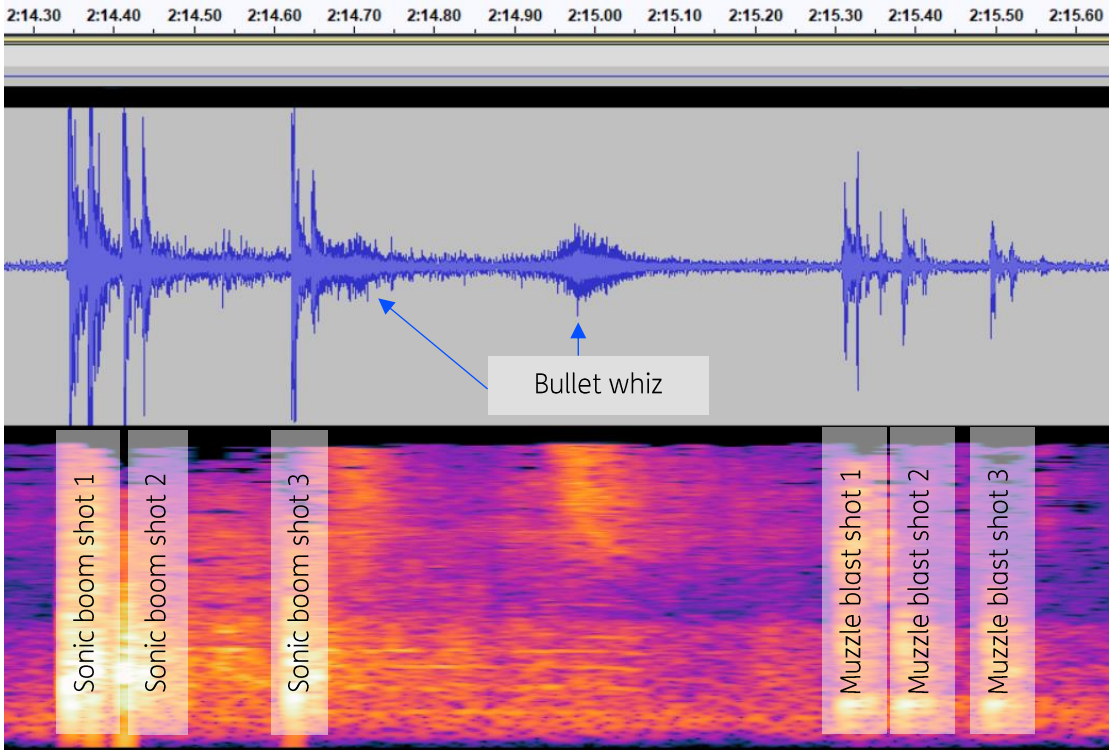

Figure 55 Arms fire consisting of three sonic booms, two bullet whizzes and three muzzle blasts.

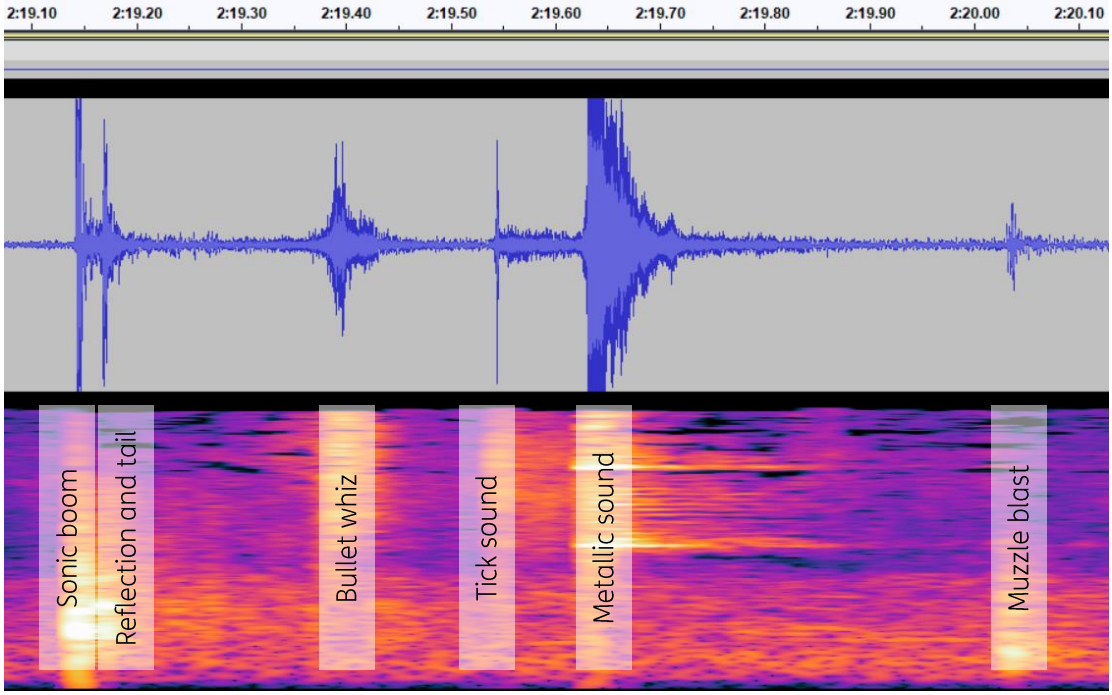

Figure 56 Arms fire consisting of a sonic boom with reflection and tail, a bullet whiz, a tick and metallic sound and a muzzle blast, all related to a single shot.

Based on the sequence of sounds in Figure 56 it is anticipated that the bullets have slowed down in flight from supersonic to subsonic speed allowing their air disturbance to be heard when passing (whizzing) by the microphone of the Al Jazeera camera at a close range.

Using a mathematical model incorporating the time of travel of the muzzle blast and of the bullet at supersonic and subsequent subsonic speed, allows for a time interval comparison against the measured sequence of sounds in Figure 55 and Figure 56. A schematic representation of the model with a supersonic and subsonic region is given in Figure 57.

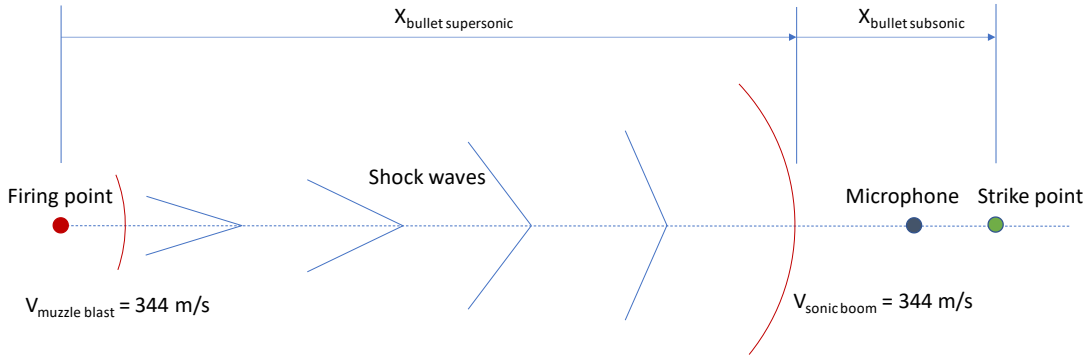

Figure 57 Schematic representation of the TNO model with a supersonic and subsonic region.

For the calculations the following assumptions are made:

- The bullet travels along a straight line as the displacement in the vertical plane is not significant over long distances (see Figure 76 in Appendix B);
- The bullet decelerates linearly with $v = v_{muzzle} + k \cdot x$, with k = deceleration coefficient in m/s/m, where in the supersonic region k is about three times higher than in the subsonic region corresponding to a supersonic/subsonic drag coefficient ratio for a .50 caliber bullet (see Figure 77 in Appendix B);
- The bullet passes the microphone of the camera at close range because the bullet can be heard passing by. The miss distance in the horizontal plane (in the subsonic region) is therefore disregarded;
- The speed of sound equals 344 m/s and potential wind effects are ignored.

A parameter study is performed using combinations of four firing distances 880, 1000, 1343 and 1500 m, two muzzle velocities 850 and 900 m/s typical for .50 caliber rounds, and a range of deceleration coefficients from -0,4 to -0,8 m/s/m[17]. The results of this study are presented in Appendix B. The only reasonable match with the time interval in Figure 55 and Figure 56 between the arrival at the microphone of the sonic boom (crack) and muzzle blast (0,89, 0,90 and 0,97 s), and the interval between the sonic boom and arrival of the bullet (0,25 and 0,35 s) is found for the combination of a firing distance of 1343 m, a muzzle velocity of 850 m/s and a linear bullet deceleration of 0.6 m/s/m[18]. This demonstrates that the machine gun fire may have originated from the same position as from where the two tank rounds were fired.

It is noted that Merkava tanks can be equipped with a M2 Heavy Barrel (HB) Browning .50 caliber machine gun, coaxial (aligned) with the tank gun and remotely controlled from within the turret [Militarytoday, 2024]. Given the short sequence of events, with arms fire about thirty seconds and one minute after the second strike, consistent with that of a .50 caliber machine gun, it is considered a likely scenario that a Merkava tank, after firing two tank rounds, also used its machine gun against the location of the journalists.

[17] A location at approximately 880 m to the southeast of the journalists was struck by a tank round fired from behind the UN 2000 Blue Line. The journalists were hit by two tank rounds fired from a distance of approximately 1343 m. k = -0,4 m/s/m is derived projectile velocities presented in [Headquarters, Department of the Army, 2019], k = -0,8 m/s/m is measured by TNO for a .50 caliber bullet with grooves.
[18] The bullet impacting the wall observed in the back of Figure 15 may have caused the metallic sound in Figure 56.

However, the latter cannot be concluded with certainty as the parameter study does not allow an accurate distance estimation and the direction of fire cannot be established based on the audio from the video camera.

4.4 Related hardware

The related hardware recovered from the scene and delivered to TNO by Reuters consists of flak vests, helmet, fragments from the Reuters car and Issam's camera, tripod and LiveU. Their analysis is detailed in the following sections.

4.4.1 Flak vests

The flak vests of Christina Assi, Dylan Collins and Issam Abdallah were visually inspected and X-rayed for detection of fragments, see Figure 58. The hard armour plates inside the flak vests have the following protection level: *Based on NIJ-0101.04 3 shots 7.62x39 AP @720 m/s max and separately 3 shots 7.62x51 brass jacket @820 m/s max on soft armour NIJ-IIIA BAP482.*

Figure 58 X-ray cabinet. A camera is used for item documentation and identification.

The images of the flak vests and corresponding X-rays are presented in Appendix C.

The flak vest of Christina Assi sustained one impact on the lower right front side without damage to the armour plate, and several impacts on the backside with minor damage to the armour plate, see Figure 78 and Figure 79. No metal fragments were found.

The flak vest of Dylan Collins sustained two impacts on the front right side without damage to the armour plate, and no impacts on the backside, see Figure 80 and Figure 81. No metal fragments were found.

The front outside and backside of the flak vest of Issam Abdallah sustained major damage. Three parts of this vest are shown in Figure 59. The individual parts with corresponding X-rays are displayed in Figure 82 and Figure 83.

Several perforations are observed in the back and front outside of the vest. Part of the Kevlar (or Aramid) has been ripped from the body armour back plate and is still present in the backside of the vest. Whether the armour plates were perforated themselves could not be determined as these plates were not obtained by TNO. No metal fragments were found.

Figure 59 Flak vest of Issam Abdallah; backside, front inside and front outside (from left to right).

4.4.2 Helmet

The helmet of Dylan Collins was visually inspected. This helmet has the following protection level: *IIIA* . No damage to the helmet was observed, see Figure 60.

Figure 60 Helmet of Dylan Collins; exterior (left) and interior (right).

4.4.3 Fragments from the Reuters car

Three fragments were removed from the Reuters car that was parked up the hill roughly ten meters away from the car that was hit. One of these fragments is shown in Figure 61. The fragments were sent by Reuters to TNO for analysis by means of SEM-EDX.

Figure 61 Fragment lodged in Reuters car.

The analysis showed that two of the fragments are made of aluminum and are covered with gravel and other metal and organic material. One fragment is made of iron and covered with silicon and calcium, presumably stemming from gravel. The fragments appeared to have a random shape.

Evidently, these fragments were projected at high velocity, but it remains unclear whether these fragments were part of the ammunition rounds that struck the location of the journalists.

4.4.4 Camera, tripod and LiveU

The Reuters camera, tripod and LiveU are displayed in Figure 62, Figure 63 and Figure 64. All three sustained damage. The camera was hit on its video display. The tripod suffered three perforations. As the LiveU pack was perforated at the top side, the pack was X-rayed. No metal fragments were found in all three items.

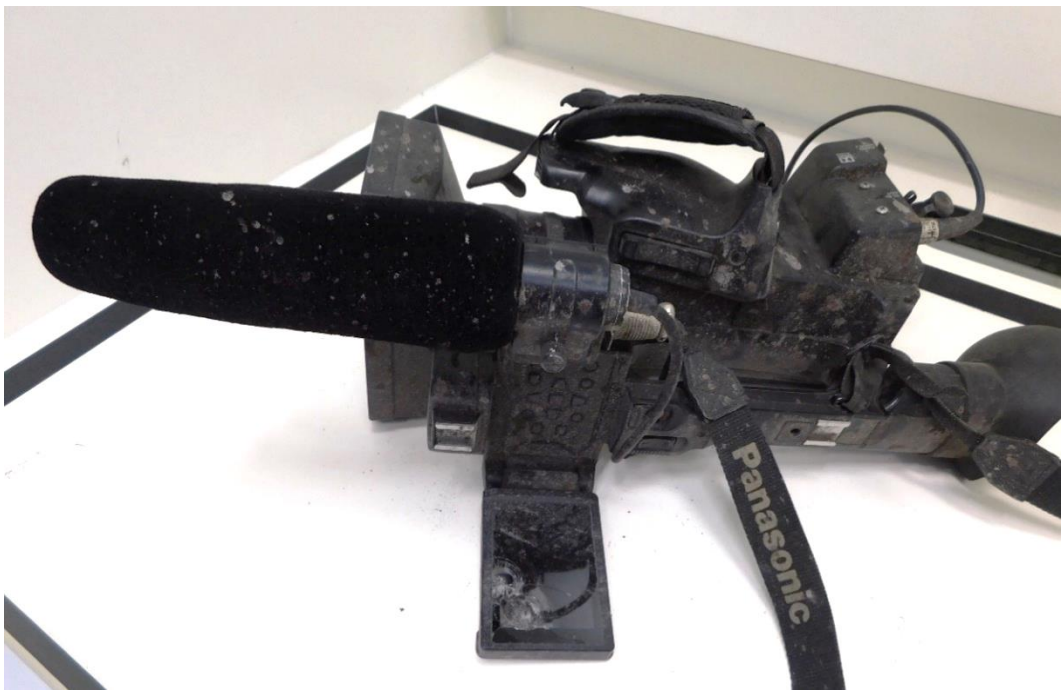

Figure 62 Reuters camera.

Figure 63 Reuters tripod.

Figure 64 Packed Reuters LiveU (left), and X-ray of pack (right). The pack was perforated at the top (near the clip).

5 Conclusions

Based on the hardware and imagery as collected by Reuters and sent by Reuters to TNO, the following conclusions are drawn:

On 13 October 2023, the journalists were present on a hilltop near Aalma el-Chaab in Lebanon for at least fifty three minutes before being struck by ammunition. They were hit around 18:02. Thirty seven seconds later they were hit again. About thirty seconds and one minute after the second strike, arms fire and bullets whizzing through the air can be heard. Throughout most of the available recordings the sound of one or more drones is audible.

Before the first strike on the journalists, ammunition was fired from behind the UN 2000 Blue Line which detonated on Lebanese soil approximately 880 m to the southeast of their location. The audio of this strike is consistent with the firing of an M329 APAM-MP-T tank round in airburst mode.

The incident location was not involved in an earlier ammunition strike. The debris pattern behind the wall hit in the first strike aligns with a firing direction from the east - southeast.

Al Jazeera audio recorded at the incident location, reveals an identical interval between the moment of strike and the muzzle blast for both strikes, which is confirmed by audio recorded by LBCI about 100 m to the southwest of the location. RAI footage demonstrates that the journalists were hit twice from the same firing point. The firing point is located behind the UN 2000 Blue Line, triangulated at 33°05'57.3"N 35°12'44.3"E, with an accuracy of +/- 17 m, and confirmed visually using landmarks in the RAI video. The terrain allows for line of sight between the firing point and the location of the journalists.

There is little doubt that a large metal piece recovered from the scene relates to the incident on 13 October 2023. This piece is identified as a tail fin assembly of a 120 mm tank round with a tracer, that was fired using a 120 mm smoothbore tank gun. The assembly matches the tail fin of a M325 HEAT-MP-T, M329 APAM-MP-T and M339 HE-MP-T produced by Elbit Systems Land. Because of their purpose and muzzle velocity comparable to the average projectile velocity calculated from the RAI footage, it is concluded that the journalists were struck by two M339 HE-MP-T rounds, two M329 APAM-MP-T rounds or a combination of both rounds, with fuzes in point detonation mode. It is anticipated that in the first strike Issam Abdallah was instantly killed by a direct hit by the round that breached the wall. For the second strike the damage to the white car is consistent with a high explosive round that detonated on the left front side of the vehicle.
The arms fire right after the second strike, with bullets passing the microphone of the Al Jazeera camera at close range, is consistent with the firing of .50 caliber ammunition from a distance similar to that of the firing point of the tank rounds. It is considered a likely scenario that a Merkava tank, after firing two tank rounds, also used its .50 caliber machine gun against the location of the journalists. The latter cannot be concluded with certainty as the direction and exact distance of fire could not be established.

No metal fragments were found in flak vests, helmet and Issam's camera, tripod and LiveU. Fragments recovered from the Reuters car could not be related to an ammunition round.

6 References

CNN, 2023
https://edition.cnn.com/2023/10/13/business/reuters-journalist-killed-lebanon/index.html (assessed on 9-11-2023)

Elbit Systems, 2023
https://elbitsystems.com/media/Catalog-Tanks_15_Web.pdf (assessed 10-11-2023)

FOB, 2023
Nexter rounds displayed at DSEI 2021, https://www.forcesoperations.com/amp/dsei-2021-de-nouvelles-munitions-nexter-pour-les-chars-daujourdhui-et-de-demain/ (assessed 30-11-2023)

GDOTS, 2023
https://www.gd-ots.com/munitions/large-caliber-ammunition/120mm-imhet/

Headquarters, Department of the Army, 2019
HEAVY MACHINE GUN M2 Series, Training Circular 3-22.50, Headquarters, Department of the Army, 19 May 2017

Moav, 2008
J. Moav, Ammunition for the changing role of the tanks in modern battlefield, Israel Military Industries Ltd. (IMI), April 2008

McCoy, 1990
R.L. McCoy, The Aerodynamic Characteristics of .50 BALL, M33, API, M8, AND APIT, M20 Ammunition, Memorandum Report Ballistic Research Laboratory-MR-3810, Aberdeen Proving Ground, Maryland, U.S. Army Laboratory Command, January 1990

Military Review, 2015
https://en.topwar.ru/69107-izrailskiy-tankovyy-snaryad-dva-v-odnom.html

Militarytoday, 2024
https://www.militarytoday.com/tanks/merkava_mk3.htm
https://www.militarytoday.com/tanks/merkava_mk4.htm (assessed 4-1-2024)

Rheinmetall, 2023
https://www.rheinmetall.com/Rheinmetall%20Group/brochure-download/Weapon-Ammmunition/B195e0423-Rheinmetall-120mm-system-house.pdf (assessed 11-12-2023)

Schirding, 2007
D. Schirding, APAM-MP-T 120mm , XM329, Israel Military Industries Ltd. (IMI), Heavy Ammunition Division, April 2007

Wikimedia Commons, 2015
https://commons.wikimedia.org/wiki/File:Hatzav-120mm-tank-cartridge.jpg (assessed 28-11-2023)

X, 2023, 1
https://twitter.com/ArmoredWar/status/1714618328629874866

YouTube, 2017
https://www.youtube.com/watch?v=R13QtP_KobU

YouTube, 2016
https://www.youtube.com/watch?v=8QVjEFK78D8

YouTube 1, 2019
https://www.youtube.com/watch?v=U61Hrn1JZWQ

YouTube 2, 2019
https://www.youtube.com/watch?v=yEAYNX_UCjw

Appendix A

Analysis of earlier strike

A.1 Geographical analysis

Approximately 45 minutes prior to the two strikes at the journalists' location, AFP cameras captured mortar fire towards the east. Figure 65 shows a screen capture from this footage [AFP Footage to the East 1.MP4]. Visible in the figure are a white and black smoke plume, indicated by blue arrows. Based on the analysis of similar footage, these plumes are assumed to be from the firing of an ammunition round from behind the UN 2000 Blue Line and its subsequent detonation on Lebanese soil. Also visible in the figure is a structure resembling an observation tower (yellow arrow). Given the direction in which the plumes are moving, and the fact that the impact happened about 10 seconds earlier, it seems likely that the this structure was the target of the strike.

Figure 65 Still from [AFP Footage to the East 1.MP4] that shows a white and black smoke plume (blue arrows), assumed to be from the firing and detonation of an ammunition round respectively. The yellow arrow indicates a tower like structure (with Mount Adir in the background).

Figure 66 shows the view of Figure 65 captured in Google Earth. The mountain top visible in the background in Figure 65 (directly behind the observation tower) can be identified as Mount Adir. Drawing a line from the filming location to Mount Adir provides the direction of the impact location. This is shown in Figure 67 and Figure 68.

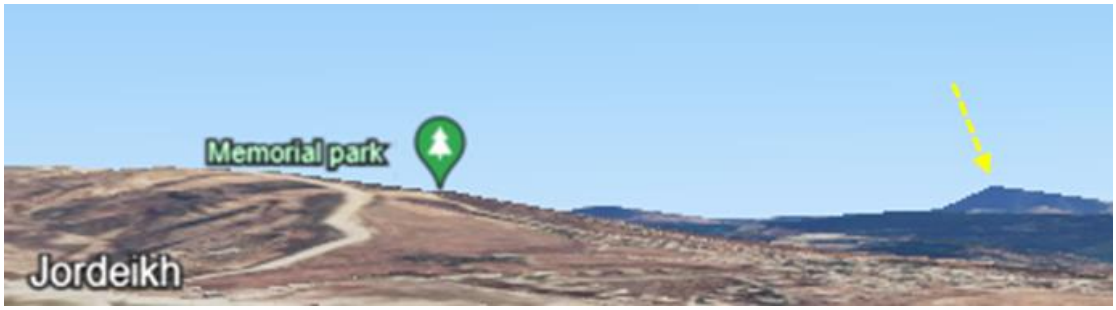

Figure 66 The view of Figure 1 captured in Google Earth. The yellow arrow indicates the top of Mount Adir.

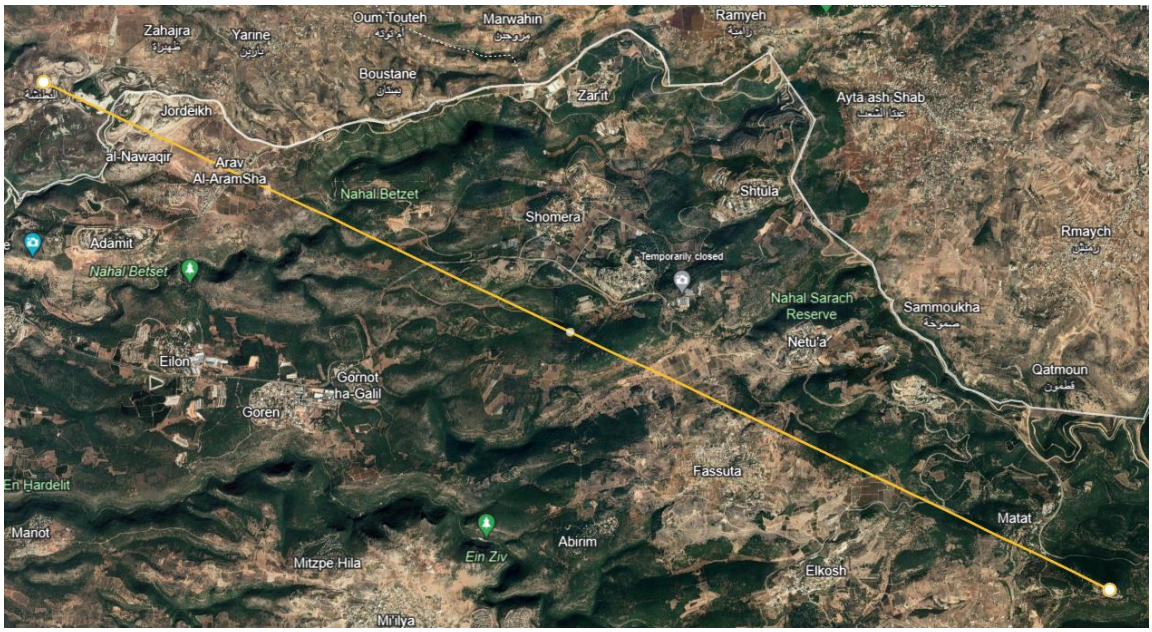

Figure 67 Line of sight from the filming location (left) to the top of Mount Adir (right).

Figure 68 Satellite view of the area, showing the filming location, the firing location, and the impact direction.

Figure 69 shows a schematic view of the information presented above. Besides the approximated firing location, the following values in this figure apply:

- x_3 = 1400 m
- α = 14 degrees
- Filming location

This leaves the following unknowns:

- x_1 (the distance between the filming location and the impact location)
- x_2 (the distance between the firing location and the impact location)

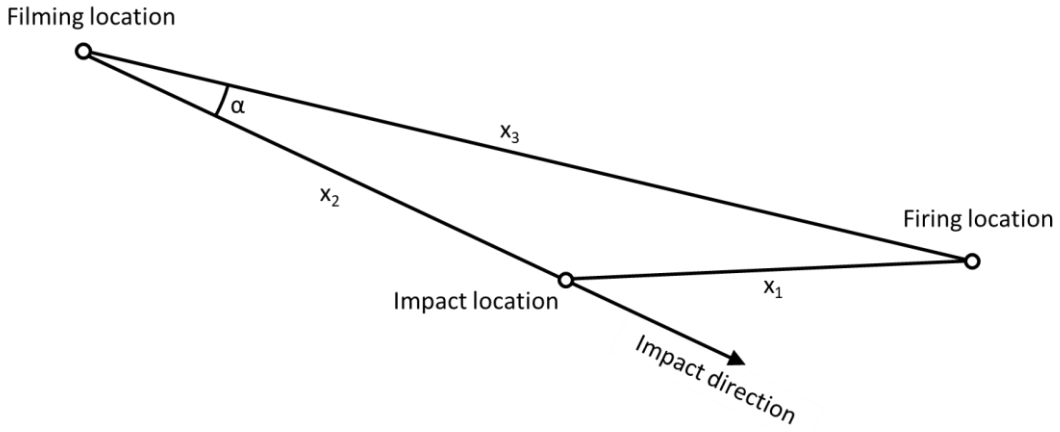

Figure 69 Schematic view of the filming location, firing location, impact location and impact direction.

In order to solve for the two unknowns x_1 and x_2, two independent equations are required. The first equation is provided by the cosine formula:

Equation 6 $$\cos\alpha = \frac{x_2^2+x_3^2-x_1^2}{2x_2x_3}$$

For the second equation, the audio from [AFP Footage to the East 1.MP4] is used. Both the sound of the impact and the sound of the muzzle blast can be heard in the video. The time difference between these two sounds provides the last piece of information needed to solve for x_1 and x_2.

A.2 Timing analysis

Based on Figure 69, the time it takes for the firing and impact sounds to reach the filming location (resp. $t_{sound,firing}$ and $t_{sound,impact}$) can be derived as follows, with the projectile launch time taken as $t = 0$:

Equation 7 $$t_{sound,firing} = \frac{x_3}{c_{air}}$$

Equation 8 $$t_{sound,impact} = \frac{x_1}{V_{proj}} + \frac{x_2}{c_{air}}$$

The difference between these points in time can be rewritten as:

Equation 9 $$\Delta t = \frac{x_3-x_2}{c_{air}} - \frac{x_1}{V_{proj}}$$

With c_{air} the velocity of sound in air and V_{proj} the velocity of the projectile. The velocity of sound was determined at 344.3 m/s (see section 3.2.2). Assuming that the projectile was of the same type as those used in the two later strikes at the filming location, the projectile velocity is set equal to 932 m/s. The value of Δt derived from the video footage, provides the second equation with x_1 and x_2 as the only unknowns. With two equations and two unknowns, the values of x_1 and x_2 can now be calculated for any given value of Δt.

A.3 Audio analysis

Figure 65 shows the audio waveform and spectrogram extracted from the footage. In the left of the figure, a cluster of six distinct pulses can be identified. This is consistent with an M329 APAM-MP-T round in airburst (AB) mode (see Table 2). In this mode, the projectile releases six submunitions detonating in quick succession (see Figure 43). Approximately one second after the detonations, the sound of the muzzle blast can be heard. Looking at the spectrogram in Figure 70, the muzzle blast can be distinguished by a low frequency pulse similar to that seen in Figure 19 and Figure 21.

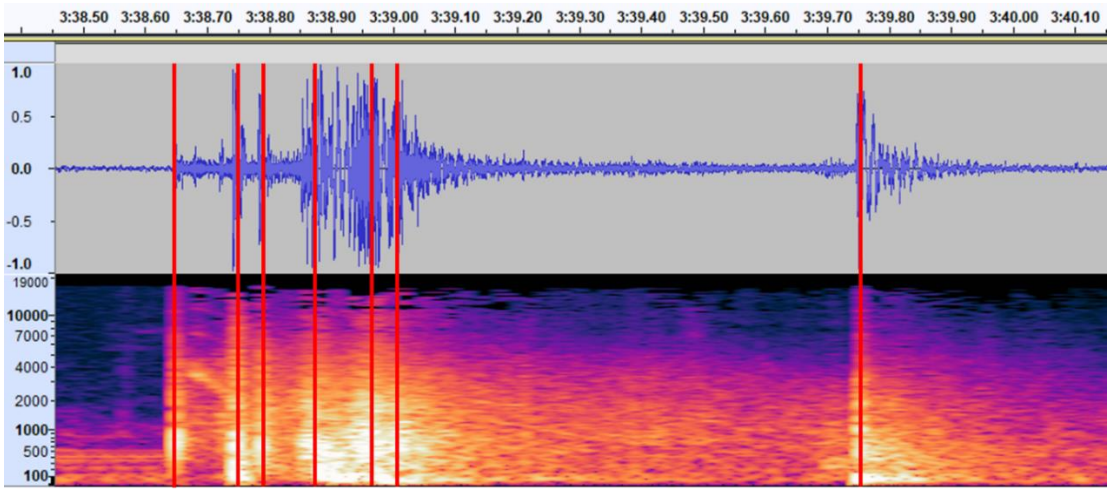

Figure 70 Audio waveform and spectrogram extracted from the AFP footage. A cluster of six pulses is heard, followed by the sound of the muzzle blast approximately one second later.

Since it is unknown which of the six detonations created the plume of black smoke on which the triangulation (as shown in Figure 69) is based, both the maximum and minimum interval are used to calculate an impact area. The maximum time interval (Δt_{max}) is the interval between the first detonation and the sound of the muzzle blast. The minimum time interval (Δt_{min}) is the interval between the last detonation and the sound of the muzzle blast. From the audio analysis it follows that:

- $\Delta t_{max} = 1.099$ s
- $\Delta t_{min} = 0.733$ s

Equation 6 and Equation 9 can now be used to calculate the values for x_1 and x_2 for both time intervals.

For $\Delta t_{max} = 1.099$ s:

- $x_1 = 771$ m
- $x_2 = 678$ m

For $\Delta t_{min} = 0.733$ s:

- $x_1 = 951$ m
- $x_2 = 532$ m

Using these values, the area in which the impact likely took place is shown in Figure 71. Figure 72 shows a more detailed view of the impact zone, which stretches across a hilltop.

Figure 71 The calculated impact location is within the red ellipse. The filming location (yellow) and firing location (blue) are also shown.

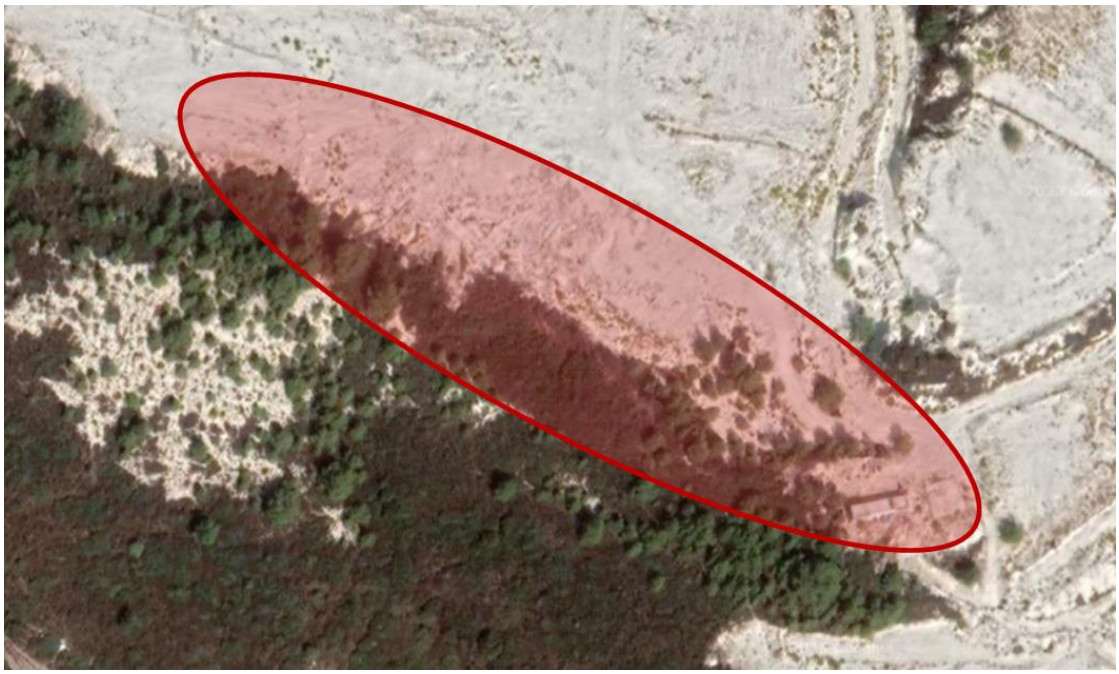

Figure 72 Zoomed in view of the calculated impact location (red ellipse).

A.4 Video analysis

In [AFP Footage to the East 2.MP4], the observation tower and its surroundings are visible in more detail. Figure 73 shows a screen capture from this footage, showing the observation tower (white frame), as well as three distinctive features of the surroundings. Figure 74 shows the same view in Google Earth, with the distinctive features from Figure 73 labelled using the same colours. The observation tower is not visible in Figure 74, but its approximate position is indicated by a white box. The blue circle in Figure 75 shows the approximate location of the observation tower, which is within the impact zone calculated based on the audio analysis (red ellipse), at approximately 880 meters from the filming location.

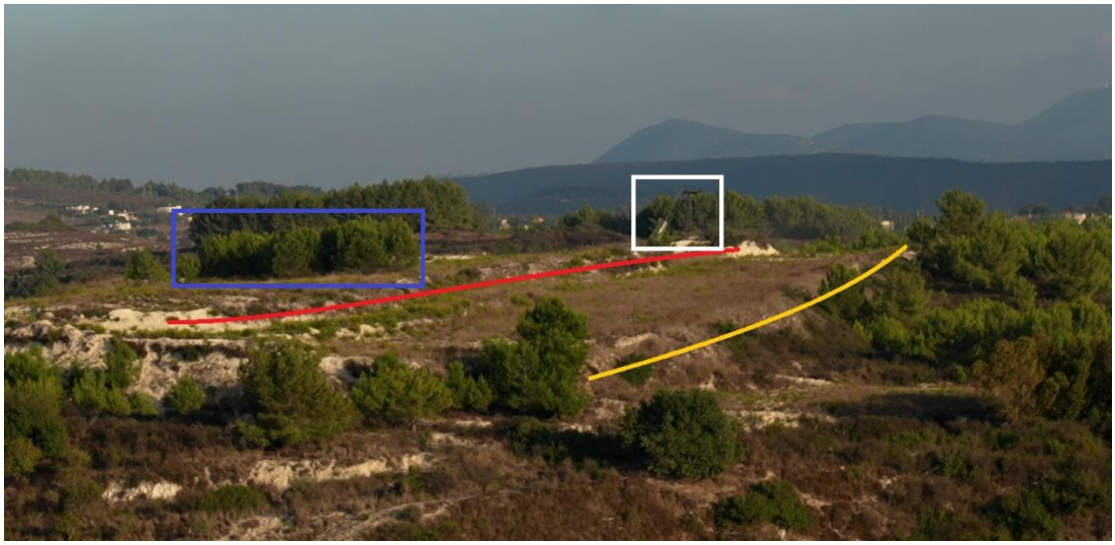

Figure 73 Screen capture from [AFP Footage to the East 2.MP4], showing the observation tower (white box), as well as other distinctive features of the surroundings.

Figure 74 The view of Figure 73 captured in Google Earth. The distinctive features from Figure 73 are labelled using the same colours. The observation tower is not visible in this figure, but its approximate position is indicated by a white box.

Figure 75 The impact location calculated from the audio analysis (red ellipse), with the approximate location of the observation tower determined from the video analysis (blue circle).

Appendix B
Arms fire parameter study

For the calculations a straight firing line is assumed as the maximum ordinate measures only a few meters over long distances, as shown in Figure 76.

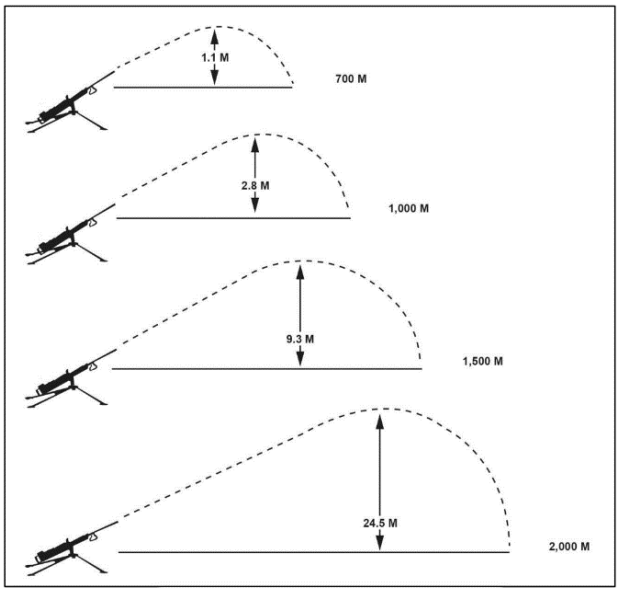

Figure 76 Maximum ordinates at key ranges [Headquarters, Department of the Army, 2019].

It is assumed that the bullet decelerates linearly with $v = v_{muzzle} + k \cdot x$, with k = deceleration coefficient in m/s/m, where in the supersonic region k is roughly three times higher than in the subsonic region corresponding to a supersonic/subsonic drag coefficient ratio for a .50 caliber bullet as shown in Figure 77. For the calculations a $CD0_{supersonic}/CD0_{subsonic}$ ratio of 0,375/0,12 is used, resulting in a factor of 3,125.

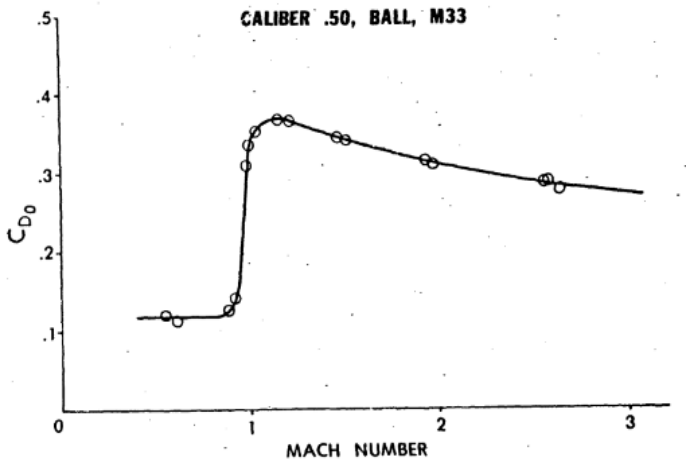

Figure 77 Zero-yaw drag force coefficient versus Mach number, Ball, M33 [McCoy, 1990].

The results of the parameter study are presented in Table 3 to Table 10. Distances are calculated using a time step of 0,01 s. The only reasonable match with the time interval in Figure 55 and Figure 56 between the arrival at the microphone of the sonic boom (crack) and muzzle blast (0,89, 0,90 and 0,97 s), and the interval between the sonic boom and arrival of the bullet (0,25 and 0,35 s) is indicated in green. Indicated with an 'x' in these tables there is no solution as the travel distance in the supersonic region is larger than the firing distance, in which case a whiz of the subsonic bullet cannot be heard (see Figure 57).

Table 3 Calculation results for x = 880 m, v_{muzzle} = 850 m/s and k = -0,4 to -0,8 m/s/m.

x firing point to microphone [m]	880	880	880	880	880	880	880	880	880
v muzzle [m/s]	850	850	850	850	850	850	850	850	850
k [m/s/m]	-0,40	-0,45	-0,50	-0,55	-0,60	-0,65	-0,70	-0,75	-0,80
x supersonic [m]	1266	1126	1010	920	842	779	724	674	634
t supersonic [s]	x	x	x	x	1,5	1,39	1,29	1,2	1,13
x subsonic [m]	x	x	x	x	38	101	156	206	246
t subsonic [s]	x	x	x	x	0,110	0,292	0,455	0,599	0,716
t arrival crack at microphone [s]	x	x	x	x	1,610	1,682	1,745	1,799	1,846
t arrival muzzle blast at microphone [s]	x	x	x	x	2,558	2,558	2,558	2,558	2,558
dt arrival crack and muzzle blast [s]	x	x	x	x	0,948	0,876	0,814	0,760	0,712
dt arrival crack and bullet [s]	x	x	x	x	0,000	0,008	0,025	0,051	0,074
x microphone to strike location [m]	x	x	x	x	40,8	39,9	39,0	38,0	37,1

Table 4 Calculation results for x = 880 m, v_{muzzle} = 900 m/s and k = -0,4 to -0,8 m/s/m.

x firing point to microphone [m]	880	880	880	880	880	880	880	880	880
v muzzle [m/s]	900	900	900	900	900	900	900	900	900
k [m/s/m]	-0,40	-0,45	-0,50	-0,55	-0,60	-0,65	-0,70	-0,75	-0,80
x supersonic [m]	1390	1235	1112	1010	927	854	795	742	696
t supersonic [s]	x	x	x	x	x	1,47	1,37	1,28	1,2
x subsonic [m]	x	x	x	x	x	26	85	138	184
t subsonic [s]	x	x	x	x	x	0,076	0,248	0,401	0,535
t arrival crack at microphone [s]	x	x	x	x	x	1,546	1,618	1,681	1,735
t arrival muzzle blast at microphone [s]	x	x	x	x	x	2,558	2,558	2,558	2,558
dt arrival crack and muzzle blast [s]	x	x	x	x	x	1,012	0,940	0,878	0,823
dt arrival crack and bullet [s]	x	x	x	x	x	0,004	0,012	0,019	0,035
x microphone to strike location [m]	x	x	x	x	x	40,9	40,1	39,1	38,2

Table 5 Calculation results for x = 1000 m, v_{muzzle} = 850 m/s and k = -0,4 to -0,8 m/s/m.

x firing point to microphone [m]	1000	1000	1000	1000	1000	1000	1000	1000	1000
v muzzle [m/s]	850	850	850	850	850	850	850	850	850
k [m/s/m]	-0,40	-0,45	-0,50	-0,55	-0,60	-0,65	-0,70	-0,75	-0,80
x supersonic [m]	1266	1126	1010	920	842	779	724	674	634
t supersonic [s]	x	x	x	1,64	1,5	1,39	1,29	1,2	1,13
x subsonic [m]	x	x	x	80	158	221	276	326	366
t subsonic [s]	x	x	x	0,233	0,459	0,641	0,803	0,947	1,065
t arrival crack at microphone [s]	x	x	x	1,873	1,959	2,031	2,093	2,147	2,195
t arrival muzzle blast at microphone [s]	x	x	x	2,907	2,907	2,907	2,907	2,907	2,907
dt arrival crack and muzzle blast [s]	x	x	x	1,034	0,948	0,876	0,814	0,760	0,712
dt arrival crack and bullet [s]	x	x	x	0,007	0,021	0,049	0,077	0,123	0,175
x microphone to strike location [m]	x	x	x	40,4	39,4	38,3	37,1	35,9	34,7

Table 6 Calculation results for x = 1000 m, v_{muzzle} = 900 m/s and k = -0,4 to -0,8 m/s/m.

x firing point to microphone [m]	1000	1000	1000	1000	1000	1000	1000	1000	1000
v muzzle [m/s]	900	900	900	900	900	900	900	900	900
k [m/s/m]	-0,40	-0,45	-0,50	-0,55	-0,60	-0,65	-0,70	-0,75	-0,80
x supersonic [m]	1390	1235	1112	1010	927	854	795	742	696
t supersonic [s]	x	x	x	x	1,6	1,47	1,37	1,28	1,2
x subsonic [m]	x	x	x	x	73	146	205	258	304
t subsonic [s]	x	x	x	x	0,211	0,425	0,597	0,749	0,884
t arrival crack at microphone [s]	x	x	x	x	1,811	1,895	1,967	2,029	2,084
t arrival muzzle blast at microphone [s]	x	x	x	x	2,907	2,907	2,907	2,907	2,907
dt arrival crack and muzzle blast [s]	x	x	x	x	1,096	1,012	0,940	0,878	0,823
dt arrival crack and bullet [s]	x	x	x	x	0,009	0,015	0,043	0,081	0,116
x microphone to strike location [m]	x	x	x	x	40,4	39,3	38,3	37,2	35,9

Table 7 Calculation results for x = 1343 m, v_{muzzle} = 850 m/s and k = -0,4 to -0,8 m/s/m.

x firing point to microphone [m]	1343	1343	1343	1343	1343	1343	1343	1343	1343
v muzzle [m/s]	850	850	850	850	850	850	850	850	850
k [m/s/m]	-0,40	-0,45	-0,50	-0,55	-0,60	-0,65	-0,70	-0,75	-0,80
x supersonic [m]	1266	1126	1010	920	842	779	724	674	634
t supersonic [s]	2,26	2,01	1,8	1,64	1,5	1,39	1,29	1,2	1,13
x subsonic [m]	77	217	333	423	501	564	619	669	709
t subsonic [s]	0,224	0,631	0,967	1,230	1,456	1,638	1,800	1,944	2,062
t arrival crack at microphone [s]	2,484	2,641	2,767	2,870	2,956	3,028	3,090	3,144	3,192
t arrival muzzle blast at microphone [s]	3,904	3,904	3,904	3,904	3,904	3,904	3,904	3,904	3,904
dt arrival crack and muzzle blast [s]	1,420	1,263	1,137	1,034	0,948	0,876	0,814	0,760	0,712
dt arrival crack and bullet [s]	0,006	0,029	0,083	0,150	0,254	0,362	0,500	0,676	0,868
x microphone to strike location [m]	40,6	39,3	37,8	36,2	34,5	32,7	30,8	28,6	26,4

Table 8 Calculation results for x = 1343 m, v_{muzzle} = 900 m/s and k = -0,4 to -0,8 m/s/m.

x firing point to microphone [m]	1343	1343	1343	1343	1343	1343	1343	1343	1343
v muzzle [m/s]	900	900	900	900	900	900	900	900	900
k [m/s/m]	-0,40	-0,45	-0,50	-0,55	-0,60	-0,65	-0,70	-0,75	-0,80
x supersonic [m]	1390	1235	1112	1010	927	854	795	742	696
t supersonic [s]	x	2,13	1,92	1,74	1,6	1,47	1,37	1,28	1,2
x subsonic [m]	x	108	231	333	416	489	548	601	647
t subsonic [s]	x	0,315	0,670	0,969	1,208	1,422	1,594	1,747	1,881
t arrival crack at microphone [s]	x	2,445	2,590	2,709	2,808	2,892	2,964	3,027	3,081
t arrival muzzle blast at microphone [s]	x	3,904	3,904	3,904	3,904	3,904	3,904	3,904	3,904
dt arrival crack and muzzle blast [s]	x	1,459	1,314	1,195	1,096	1,012	0,940	0,878	0,823
dt arrival crack and bullet [s]	x	0,005	0,040	0,091	0,162	0,258	0,376	0,513	0,679
x microphone to strike location [m]	x	40,3	38,9	37,4	35,8	34,1	32,3	30,2	28,1

Table 9 Calculation results for x = 1500 m, v_{muzzle} = 850 m/s and k = -0,4 to -0,8 m/s/m.

x firing point to microphone [m]	1500	1500	1500	1500	1500	1500	1500	1500	1500
v muzzle [m/s]	850	850	850	850	850	850	850	850	850
k [m/s/m]	-0,40	-0,45	-0,50	-0,55	-0,60	-0,65	-0,70	-0,75	-0,80
x supersonic [m]	1266	1126	1010	920	842	779	724	674	634
t supersonic [s]	2,26	2,01	1,8	1,64	1,5	1,39	1,29	1,2	1,13
x subsonic [m]	234	374	490	580	658	721	776	826	866
t subsonic [s]	0,680	1,087	1,423	1,686	1,912	2,095	2,257	2,401	2,518
t arrival crack at microphone [s]	2,940	3,097	3,223	3,326	3,412	3,485	3,547	3,601	3,648
t arrival muzzle blast at microphone [s]	4,360	4,360	4,360	4,360	4,360	4,360	4,360	4,360	4,360
dt arrival crack and muzzle blast [s]	1,420	1,263	1,137	1,034	0,948	0,876	0,814	0,760	0,712
dt arrival crack and bullet [s]	0,030	0,093	0,187	0,314	0,468	0,655	0,883	1,169	1,521993
x microphone to strike location [m]	39,3	37,7	35,9	34,0	31,9	29,7	27,2	24,5	21,5

Table 10 Calculation results for x = 1500 m, v_{muzzle} = 900 m/s and k = -0,4 to -0,8 m/s/m.

x firing point to microphone [m]	1500	1500	1500	1500	1500	1500	1500	1500	1500
v muzzle [m/s]	900	900	900	900	900	900	900	900	900
k [m/s/m]	-0,40	-0,45	-0,50	-0,55	-0,60	-0,65	-0,70	-0,75	-0,80
x supersonic [m]	1390	1235	1112	1010	927	854	795	742	696
t supersonic [s]	2,4	2,13	1,92	1,74	1,6	1,47	1,37	1,28	1,2
x subsonic [m]	110	265	388	490	573	646	705	758	804
t subsonic [s]	0,319	0,771	1,127	1,426	1,665	1,879	2,051	2,203	2,337
t arrival crack at microphone [s]	2,719	2,901	3,047	3,166	3,265	3,349	3,421	3,483	3,537
t arrival muzzle blast at microphone [s]	4,360	4,360	4,360	4,360	4,360	4,360	4,360	4,360	4,360
dt arrival crack and muzzle blast [s]	1,641	1,459	1,314	1,195	1,096	1,012	0,940	0,878	0,823
dt arrival crack and bullet [s]	0,011	0,049	0,113	0,214	0,335	0,501	0,689	0,927	1,223
x microphone to strike location [m]	40,4	38,8	37,1	35,3	33,4	31,2	28,9	26,3	23,6

Appendix C
Flak vests

The front and back side of the vest and armour plate of Christina Assi, with corresponding X-ray images, are shown in Figure 78 and Figure 79.

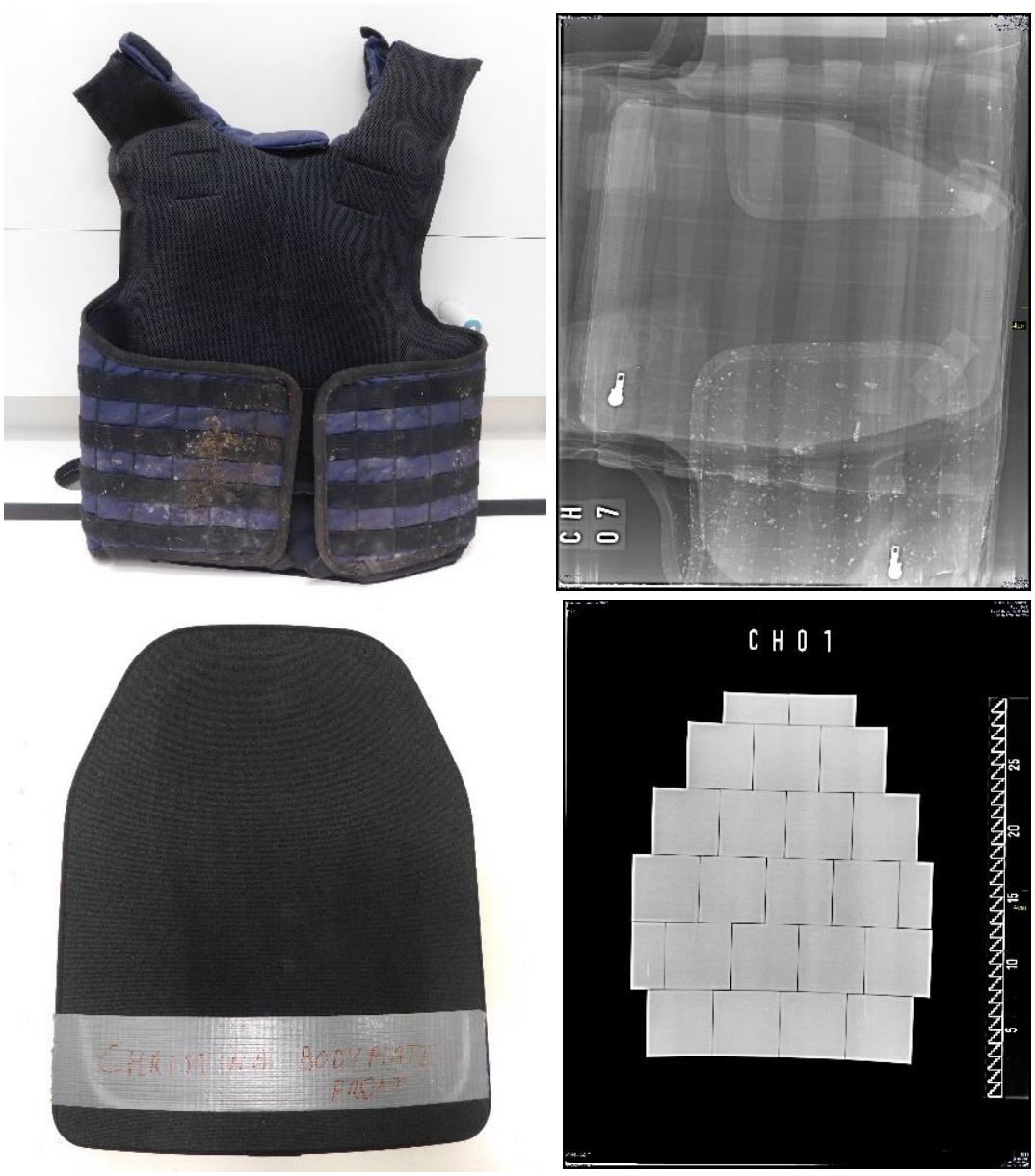

Figure 78 Frontside of body vest and armour plate of Christina Assi, with corresponding X-ray images.

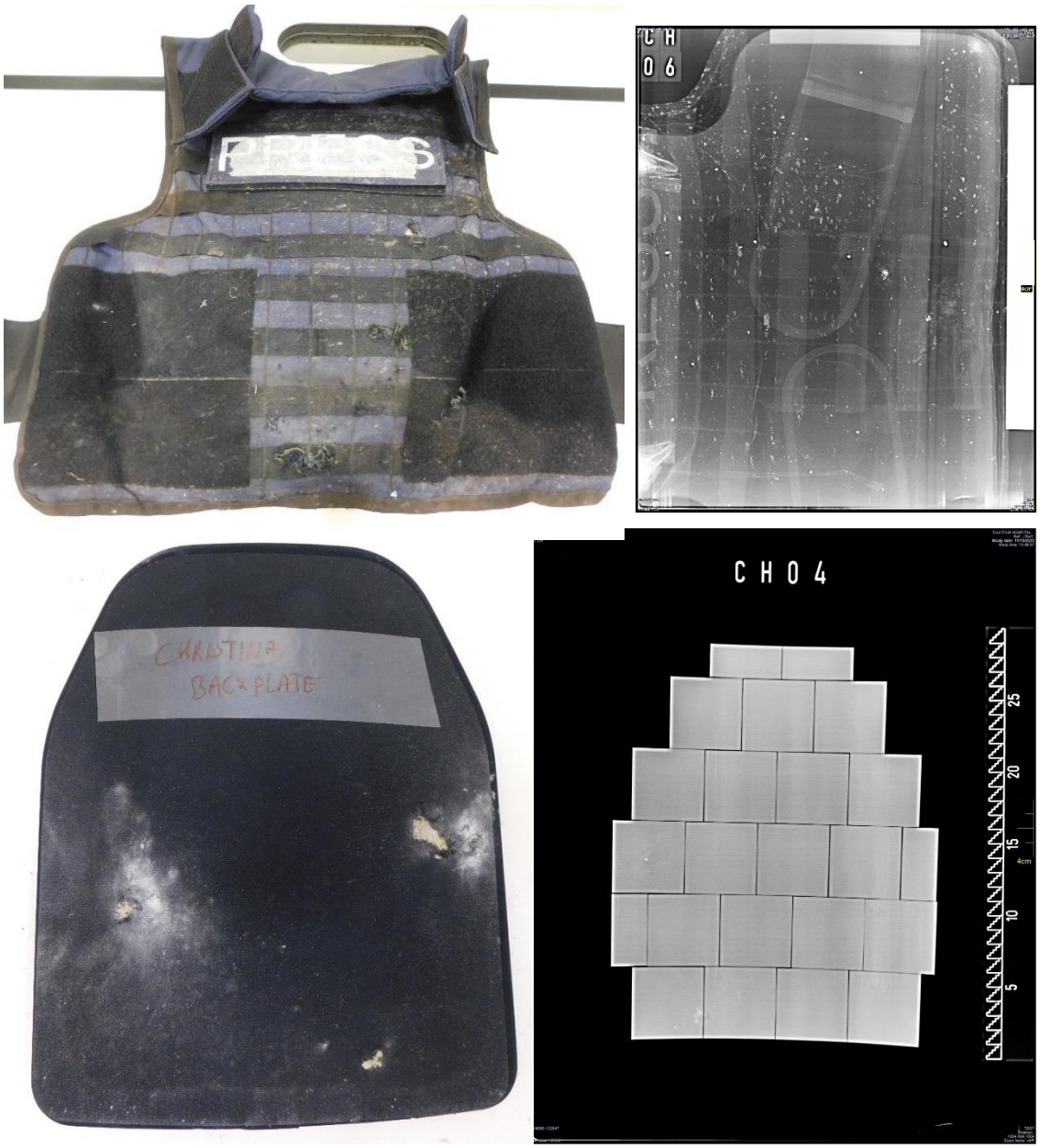

Figure 79 Backside of body vest and armour plate of Christina Assi, with corresponding X-ray images.

The front and back side of the vest and armour plate of Dylan Collins, with corresponding X-ray images, are shown in Figure 80 and Figure 81.

Figure 80 Frontside of body vest and armour plate of Dylan Collins, with corresponding X-ray images.

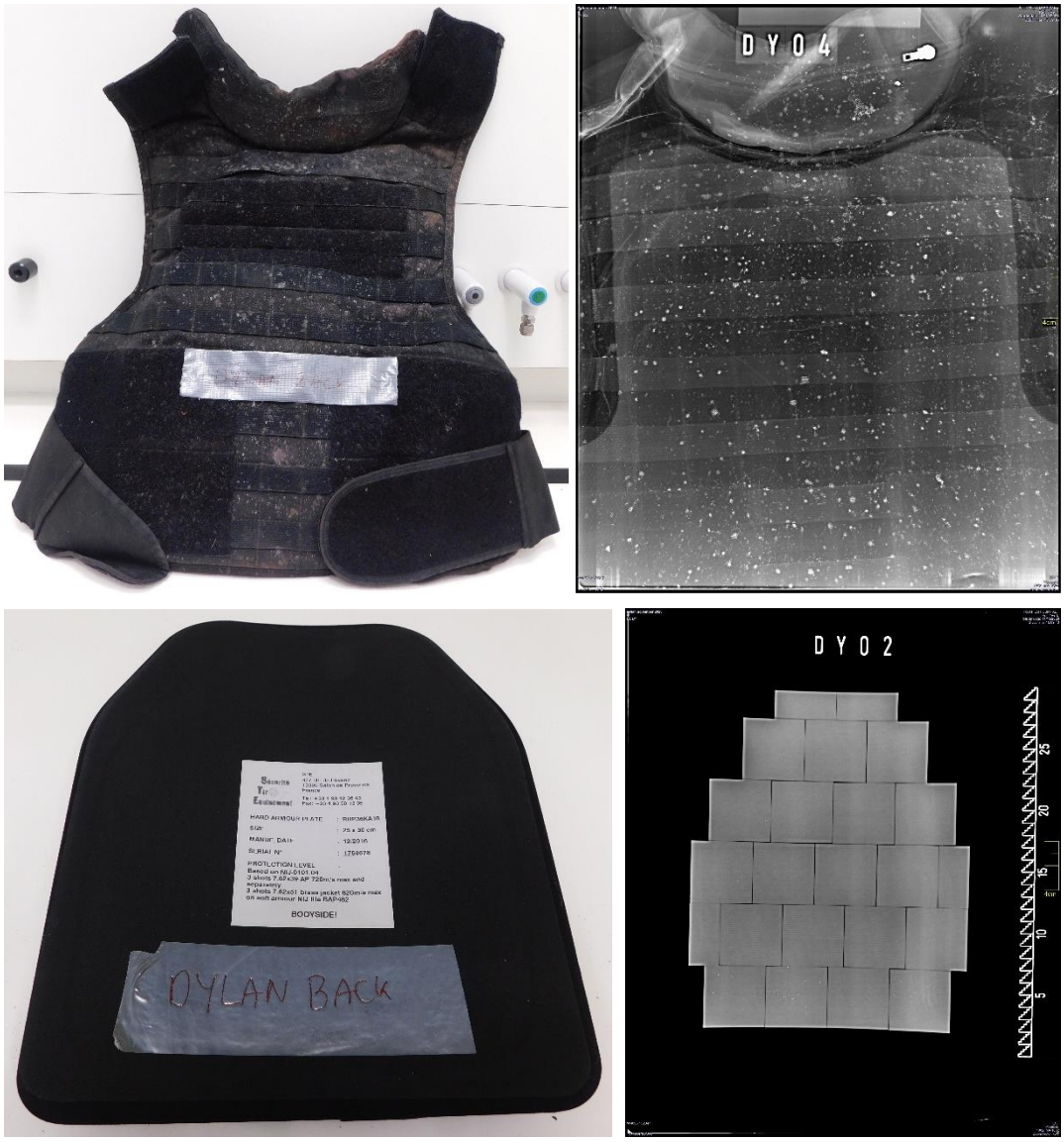

Figure 81 Backside of body vest and armour plate of Dylan Collins, with corresponding X-ray images.

The front inside and outside of the vest of Issam Abdallah, with corresponding X-ray images, are shown in Figure 82. The backside of the vest is shown in Figure 83.

Figure 82 Front inside and outside of the vest of Issam Abdallah, with corresponding X-ray images.

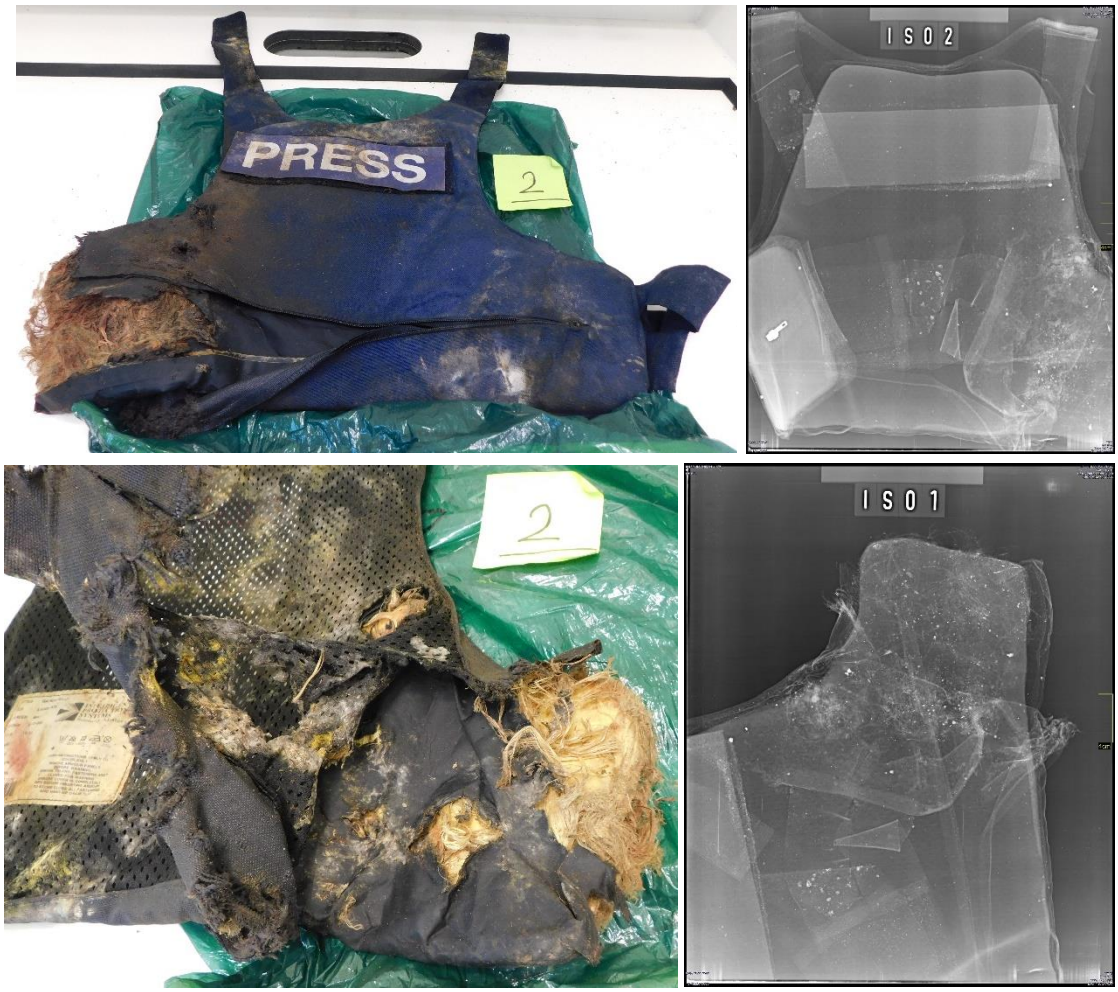

Figure 83 Backside of the vest of Issam Abdallah, with corresponding X-ray images.

Defence, Safety & Security

Ypenburgse Boslaan 2
2496 ZA Den Haag
www.tno.nl

TNO innovation for life